

# **Evaluation of the WaPOR v3 Dataset for Crop Water Productivity and Precision Agriculture Applications**

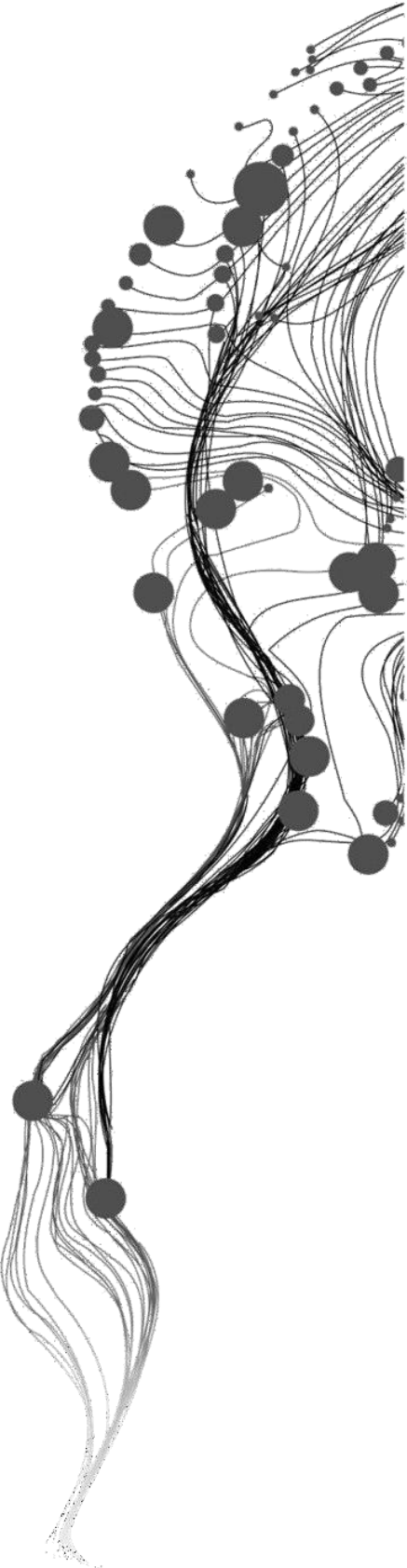
Kaan Er

June, 2024

SUPERVISORS:

Dr. Egor Prikaziuk

Dr.ir, Christiaan van der Tol



# Evaluation of the WaPOR v3 Dataset for Crop Water Productivity and Precision Agriculture Applications

Kaan Er

Enschede, The Netherlands, June, 2024

Thesis submitted to the Faculty of Geo-Information Science and Earth Observation of the University of Twente in partial fulfilment of the requirements for the degree of Master of Science in Geo-information Science and Earth Observation.

Specialization: Water Resources and Environmental Management

**SUPERVISORS:**

Dr. Egor Prikaziuk

Dr.ir, Christiaan van der Tol

**THESIS ASSESSMENT BOARD:**

Dr.ir, S. Salama (Chair)

Dr. M.T Marshall (External Examiner, University of Twente)

#### DISCLAIMER

This document describes work undertaken as part of a programme of study at the Faculty of Geo-Information Science and Earth Observation of the University of Twente. All views and opinions expressed therein remain the sole responsibility of the author, and do not necessarily represent those of the Faculty.

## ABSTRACT

This study evaluates the reliability and performance of the Water Productivity Open-access portal (WaPOR) version 3 dataset for its application in precision agriculture across various European countries. Given the increasing importance of optimizing water usage in agriculture to ensure sustainable practices, the focus is on the accuracy of WaPOR v3 in estimating Net Primary Productivity (NPP) and Actual Evapotranspiration and Interception (AETI). The study employs remote sensing methods to compute gross biomass water productivity (GBWP) and assesses water use efficiency by utilizing eddy covariance data. The results provide valuable insights into the reliability of the dataset and offer information on its applicability for precision and sustainable agriculture. This assessment underscores the dataset's potential to support effective agricultural planning and water resource management.

**Keywords:** WaPOR v3, Eddy Covariance, Precision Agriculture, Precision Agriculture Technology, Remote Sensing, Net Primary Productivity (NPP), Actual Evapotranspiration and Interception (AETI), Gross Biomass Water Productivity (GBWP), Sustainable Agriculture, Water Use Efficiency.

## ACKNOWLEDGMENTS

Firstly, I would like to express my gratitude to the Republic of Turkey Ministry of Education and the Republic of Turkey Ministry of Agriculture and Forestry for providing me this scholarship and opportunity.

I would like to thank my primary supervisor, Dr. Egor Prikaziuk, for his unwavering support, guidance, and assistance. Additionally, I would like to thank to my second supervisor, Dr. Christiaan van der Tol, for his valuable contributions.

I would like to express my grateful to my future spouse, Deniz, and my sister Dilan for their support and help. Furthermore, I would like to thank all my friends, especially Onur and Indupriya.

Bana bu zamanki destekleri için sevgili anneme ve babama, ayrıca burada olmamda büyük pay sahibi olan teyzem İpek'e ve kuzenim Özge'ye sonsuz teşekkürlerimi sunuyorum.

## ETHICAL CONSIDERATION

This study used only open-access data, ensuring no private or sensitive information was involved. No individual's privacy rights were violated, and all data usage complied with ethical and legal standards. Additionally, all the previous studies this research built upon were properly referenced in the body of the text and the reference list.

## **CONTENTS**

LIST OF FIGURES.....	viii
LIST OF TABLE .....	x
1. Introduction .....	1
1.1 Motivation and Importance.....	1
1.2 Background and Related Work.....	2
1.3 Problem Identification .....	3
2. Objectives and research questions.....	4
2.1. Overall objective .....	4
2.2. Sub-objectives .....	4
2.3 Research questions.....	4
3. Study area.....	5
4. Methodology .....	7
4.1 Eddy Covariance Method .....	9
4.2 WaPOR .....	10
4.2.1 Actual Evapotranspiration and Interception (AETI).....	10
4.2.2 Net Primary Productivity (NPP) .....	11
4.3 Phenology .....	12
4.4 Seasonal Aggregation.....	13
4.5 Gross Biomass Water Productivity (GBWP) Calculation .....	13
4.6 Accuracy Assessment .....	14
5. Results .....	16
5.1 Dekadal Data .....	16
5.1.1 Pixel Position Uncertainty.....	16
5.1.2 Dekadal Patterns .....	19
5.1.3 Special case: Station FR_Aur.....	21
5.1.4 Accuracy Metrics.....	22
5.2 Seasonal Aggregation .....	23
5.2.1 Start of the season and end of the season uncertainty.....	23
5.2.2 Total biomass.....	25
5.2.3 Water consumption.....	26
5.3 Gross Biomass Water Productivity.....	28
6. Discussion.....	30
7. Conclusion .....	32

Appendix A .....	33
A.1 Dekadal Pattern for Phenology Retrieval.....	33
A.2 Gross Biomass Water Productivity .....	36
References.....	43



## **LIST OF FIGURES**

Figure 1. Study Area Map .....	6
Figure 2 Dekadal data workflow .....	7
Figure 3. Seasonal value workflow .....	8
Figure 4. Pixel position map for BE_Lon.....	16
Figure 5.Pixel position map for CZ_KrP .....	17
Figure 6. Pixel position map for DE_Geb .....	17
Figure 7. Pixel position map for DE_Kli .....	17
Figure 8. Pixel position map for DE_Rus .....	18
Figure 9. Pixel position map for FR_Aur.....	18
Figure 10. Pixel position map for FR_Lam.....	18
Figure 11. Comparison of NPP (left) and ET (right) between WaPOR and EC tower measurements for BE_Lon.....	19
Figure 12. Comparison of NPP (left) and ET (right) between WaPOR and EC tower measurements for CZ_KrP .....	19
Figure 13. Comparison of NPP (left) and ET (right) between WaPOR and EC tower measurements for DE_Geb .....	20
Figure 14. Comparison of NPP (left) and ET (right) between WaPOR and EC tower measurements for DE_Kli .....	20
Figure 15. Comparison of NPP (left) and ET (right) between WaPOR and EC tower measurements for DE_RuS.....	20
Figure 16. Comparison of NPP (left) and ET (right) between WaPOR and EC tower measurements for FR_Aur.....	21
Figure 17. Comparison of NPP (left) and ET (right) between WaPOR and EC tower measurements for FR_Lam .....	21
Figure 18. NPP WaPOR and NPP Flux with NDVI for FR_Aur .....	22
Figure 19. The start of the season (left) and end of the season (right) of NPP WaPOR and NPP Flux .....	24
Figure 20. Comparison of Total Biomass Distrubution: EC Days (Left) vs. WaPOR Days (Right).....	25
Figure 21. Comparison of Total Biomass with respective dates.....	26
Figure 22. Distrubition of WC values of WaPOR and Flux with EC days (Left) and WaPOR days (Right) .....	27
Figure 23. Distribution of WC values of WaPOR and Flux with Flux dates.....	27
Figure 24. GBWP Flux vs WaPOR with EC towers dates (left) and WaPOR dates (right) ....	28
Figure 25. GBWP Flux vs WaPOR with respective dates.....	29

## APPENDIX

Figure A 1. Comparison of NPP (WaPOR vs. Flux) on the left and ET (WaPOR vs. Flux) on the right, with thresholds for BE_Lon.....	33
Figure A 2. Comparison of NPP (WaPOR vs. Flux) on the left and ET (WaPOR vs. Flux) on the right, with thresholds for CZ_KrP.....	33
Figure A 3. Comparison of NPP (WaPOR vs. Flux) on the left and ET (WaPOR vs. Flux) on the right, with thresholds for DE_Geb .....	34
Figure A 4. Comparison of NPP (WaPOR vs. Flux) on the left and ET (WaPOR vs. Flux) on the right, with thresholds for DE_Kli .....	34
Figure A 5. Comparison of NPP (WaPOR vs. Flux) on the left and ET (WaPOR vs. Flux) on the right, with thresholds for DE_RuS .....	34
Figure A 6. Comparison of NPP (WaPOR vs. Flux) on the left and ET (WaPOR vs. Flux) on the right, with thresholds for FR_Aur.....	35
Figure A 7. Comparison of NPP (WaPOR vs. Flux) on the left and ET (WaPOR vs. Flux) on the right, with thresholds for FR_Lam .....	35

## **LIST OF TABLE**

Table 1.Study Area .....	5
Table 2. Accuracy Metrics for NPP.....	22
Table 3. Accuracy Metrics for ET.....	23
Table 4. The day difference for SOS between Flux and WaPOR.....	24
Table 5. The day difference for EOS between Flux and WaPOR .....	24

### APPENDIX

Table A 1.GBWP values with Flux dates for BE_Lon.....	36
Table A 2.GBWP values with WaPOR dates for BE_Lon.....	36
Table A 3.GBWP values with their respective dates for BE_Lon .....	36
Table A 4 .GBWP values with Flux dates for CZ_KrP .....	37
Table A 5. GBWP values with WaPOR dates for CZ_KrP .....	37
Table A 6 .GBWP values with their respective for CZ_KrP.....	37
Table A 7.GBWP values with Flux dates for DE_Geb.....	38
Table A 8.GBWP values with WaPOR dates for DE_Geb.....	38
Table A 9.GBWP values with their respective for DE_Geb .....	38
Table A 10.GBWP values with Flux dates for DE_Kli .....	39
Table A 11.GBWP values with WaPOR dates for DE_Kli.....	39
Table A 12.GBWP values with respective dates for DE_Kli.....	39
Table A 13.GBWP values with Flux dates for DE_RuS.....	40
Table A 14.GBWP values with WaPOR dates for DE_RuS.....	40
Table A 15. GBWP values with respective dates for DE_RuS.....	40
Table A 16.GBWP values with Flux dates for FR_Aur.....	41
Table A 17.GBWP values with WaPOR dates for FR_Aur.....	41
Table A 18.GBWP values with respective dates for FR_Aur.....	41
Table A 19.GBWP values with Flux dates for FR_Lam .....	42
Table A 20.GBWP values with WaPOR dates for FR_Lam .....	42
Table A 21.GBWP values with respective dates for FR_Lam .....	42

# 1. INTRODUCTION

## 1.1 Motivation and Importance

The importance of crop water productivity lies in producing more food with less water, which helps ensure sustainable agriculture. The idea of improving farming by using water more wisely is captured by the concept that proposes the possibility of increased production of rainfed crops per unit of water used. This idea is commonly stated as the goal of “more crop per drop” (Blum, 2009). Scientists’ definition of 'crop per drop' varies, but we can define it as 'more production per unit of evapotranspiration (ET). This term has become important for sustainable agriculture (Molden et al., 2003). By 2050, the global population will approach 10 billion, significantly increasing the demand for vital resources such as food, feed, fiber, and biofuels. Agriculture plays a critical role in meeting these needs sustainably and efficiently. It stands as a cornerstone for meeting these escalating demands in a manner that is not only economically viable but also environmentally sustainable and socially beneficial (Nations et al., 2019).

Agriculture currently consumes the most water worldwide and uses one-third of the Earth's land area. With increasing competition for these resources, optimizing their use becomes imperative (FAO, 2020). The increasing demand for food and the limited availability of water resources have increased the urgency for implementing sustainable agricultural practices that enhance crop water productivity (GBWP) (Blatchford et al., 2019).

Optimizing both inputs and outputs is essential for sustainability. Simply achieving high yields does not ensure sustainability; rather, it is the efficient management of resources that leads to sustainable agricultural practices. (Tilman et al., 2011). Therefore, Farmers strive to optimize their agricultural practices to achieve higher crop yields while minimizing water consumption (*Water for Sustainable Food and Agriculture A Report Produced for the G20 Presidency of Germany*, n.d.). It is essential to increase water productivity to maintain long-term food security due to the growing demand for water resources and continued demand for food and fiber (Bossio et al., 2010). Achieving global food security has emerged as one of the biggest challenges in the 21st century, largely due to the detrimental effects of climate change on agricultural systems (Zhang et al., 2023). Although high efficiency is very important in agricultural production, it does not cover the entire sustainable agriculture. Sustainable practices involve rational management and optimization of resources (Cassman, 1999).

Although this study uses water as the input, precision agriculture technologies enable the measurement and optimization of various agricultural inputs and outputs, such as fertilizers, pesticides, and machinery, to achieve an optimal balance in farming practices (Balafoutis et al., 2017).

Smart sensors and IoT devices provide real-time data on soil moisture, crop health, and environmental conditions, enabling precise application of water, fertilizers, and pesticides. This reduces waste and minimizes the environmental impact of farming practices (Soussi et al., 2024). Additionally, advancements in agricultural machinery, such as GPS-guided tractors and drones, support precise field operations, from planting to harvesting. The integration of these technologies supports the development of a sustainable and smart agriculture system, ensuring efficient use of resources and optimized agricultural outputs (Karunathilake et al., 2023).

Monitoring and forecasting local crop production are critical steps in addressing food security problems at a global scale (Huang et al., 2019). In the context of this study, the

focus is on computing water productivity (WP) through the utilization of remote sensing methods and the assessment of water use efficiency in agriculture.

Owing to time-series remote sensing data, we have the opportunity to produce maps of water productivity ( $\text{kg}/\text{m}^3$ ) over large areas (Bastiaanssen & Bos, 1999). This research aims to contribute to sustainable agricultural practices by addressing the issue of water scarcity in agriculture and examining the relationship between water use and crop productivity. By exploring and evaluating the crop water productivity dataset provided by the Food and Agriculture Organization's Water Productivity Open-access portal (WaPOR), this study assesses the dataset's accuracy and usefulness for decision-makers involved in water resource management and agricultural planning.

## **1.2 Background and Related Work**

Researchers and policymakers alike have focused on developing and implementing strategies to maximize crop yields while minimizing water usage. Additionally, some studies have been done to determine the best irrigation methods.

A notable contribution to the field is the study by (Hellegers et al., 2009). This article demonstrates the effectiveness of using remote sensing combined with socio-economic analysis to model changes in water productivity. It is claimed that by understanding the benefits of allocating water in a more optimal way rather than a more productive one, a basis for arguments on water transfer can be significantly strengthened and made more objective. The study's findings show that remote sensing can be used to validate historical water consumption rates and evaluate spatial and temporal variations in crop water productivity analysis.

Furthermore, (Blatchford et al., 2019) evaluated the accuracy of WP products that were both satellite-driven and in-situ measured. The study evaluated the relative error range of the WP using remote sensing under the best-case scenario. The results showed that remote sensing could predict WP with a similar error range to in situ techniques. However, further research is needed to close the gap between remote sensing estimates of gross primary productivity (GPP) and crop production because there is a lot of uncertainty in the intermediates that convert GPP into yield.

A recent study by (Safi et al., 2022) introduces a standardized approach using open-source remote sensing data to diagnose crop water productivity (WP) variations. Applied to the Bekaa Valley in Lebanon, the study examines wheat, potato, and table grapes, identifying six key factors influencing WP and yield: crop water stress, irrigation uniformity, soil salinity, nitrogen application, crop rotation, and soil type. It finds that wheat and potato growth suffers from water stress during critical growth stages, non-uniform irrigation, and nitrogen stress. Additionally, potatoes on clay-loam soil perform better in WP and yield than those on loam soil. This framework helps identify priority areas and actions for improving WP at the crop field level, despite the inherent uncertainties in remote sensing data.

### **1.3 Problem Identification**

The WaPOR 2.1 portal, which was the comprehensive data set consisting of estimates of Net Primary Productivity (NPP) and actual evapotranspiration and interception (AETI) in near real-time for the African continent, covering the period from 2009 to the present (FAO and IHE Delft, 2020b). The newly developed WaPOR version 3 provides these data globally. It is important to address the validation of WaPOR v3 to ensure the accuracy and reliability of this dataset, particularly for agriculture monitoring. Therefore, it is essential to thoroughly validate WaPOR v3 to evaluate the quality of the dataset and establish its credibility for precise GBWP calculations.

## **2. OBJECTIVES AND RESEARCH QUESTIONS**

### **2.1. Overall objective**

The main aim of this study is to evaluate and compare the reliability and performance of the WaPOR v3 dataset in the context of the European countries. The primary focus is to conduct a comprehensive evaluation of WaPOR v3 compared to field data, aiming to provide information on its accuracy and suitability for data application.

### **2.2. Sub-objectives**

SO.1) Evaluate the quality of WaPOR data for estimating Net Primary Productivity (NPP) and Actual Evapotranspiration and interception (AETI)

SO. 2) Retrieve SOS and EOS to produce seasonally aggregated values

SO. 3) Validate seasonally aggregated values of total biomass and water consumption

SO. 4) Calculate and validate gross biomass water productivity (GBWP)

### **2.3 Research questions**

RQ1: How well do dekadal NPP Data in WaPOR v3 agree with in-situ measurements?

RQ2: How well do dekadal AETI Data in WaPOR v3 agree with in-situ measurements?

RQ3: How much does the uncertainty in SOS and EOS affect the agreement of seasonally aggregated values?

RQ4: Is the quality of WaPOR v3 sufficient to calculate gross biomass water productivity (GBWP)?

### 3. STUDY AREA

Eddy covariance data from seven cropland fields from the Integrated Carbon Observation System (ICOS) Warm Winter 2020 dataset (<https://doi.org/10.18160/2G60-ZHAK>) were used in the study. These fields are located in Belgium, Germany, France Czech Republic (Figure 1). A detailed description of each station is given below in Table 1. The information regarding the stations in this study was obtained from the Integrated Carbon Observation System website (<https://www.icos-cp.eu/data-products/2G60-ZHAK>). There were two more cropland stations in the dataset in Switzerland (CH\_Oe2), and Finland (FI\_Qvd), which did not have NPP or ET flux values thus were excluded from the analysis.

*Table 1. Study Area*

Code	Country	Coordinates	Area	Crop Type
BE_Lon	Belgium	50.55° N, 4.74° E	11.8 ha (300x400 m <sup>2</sup> )	Sugar beet, winter wheat, potato, and winter wheat
CZ_KrP	Czech Republic	49.57° N, 15.07° E		
DE_Geb	Germany	51.09° N, 10.91° E	33.75 ha (500x675 m <sup>2</sup> )	Winter wheat, potato, rape, peppermint, winter barley, sugar beet, durum wheat, and spring wheat
DE_Kli	Germany	50.89° N, 13.52° E	29.7 ha (990x300 m <sup>2</sup> )	Winter wheat, forage maize, spring barley, winter barley, and catch crop
DE_Rus	Germany	50.86° N, 6.44° E	8 ha (350x 230 m <sup>2</sup> )	Rapeseed, potatoes, maize oats, and white mustard.
FR_Aur	France	43.54° N, 1.10° E	23.5 ha	Wheat, rapeseed, winter wheat, sunflower, and winter cover crops
FR_Lam	France	43.49° N, 1.23° E	22.5 ha (480x470 m <sup>2</sup> )	Maize and winter wheat



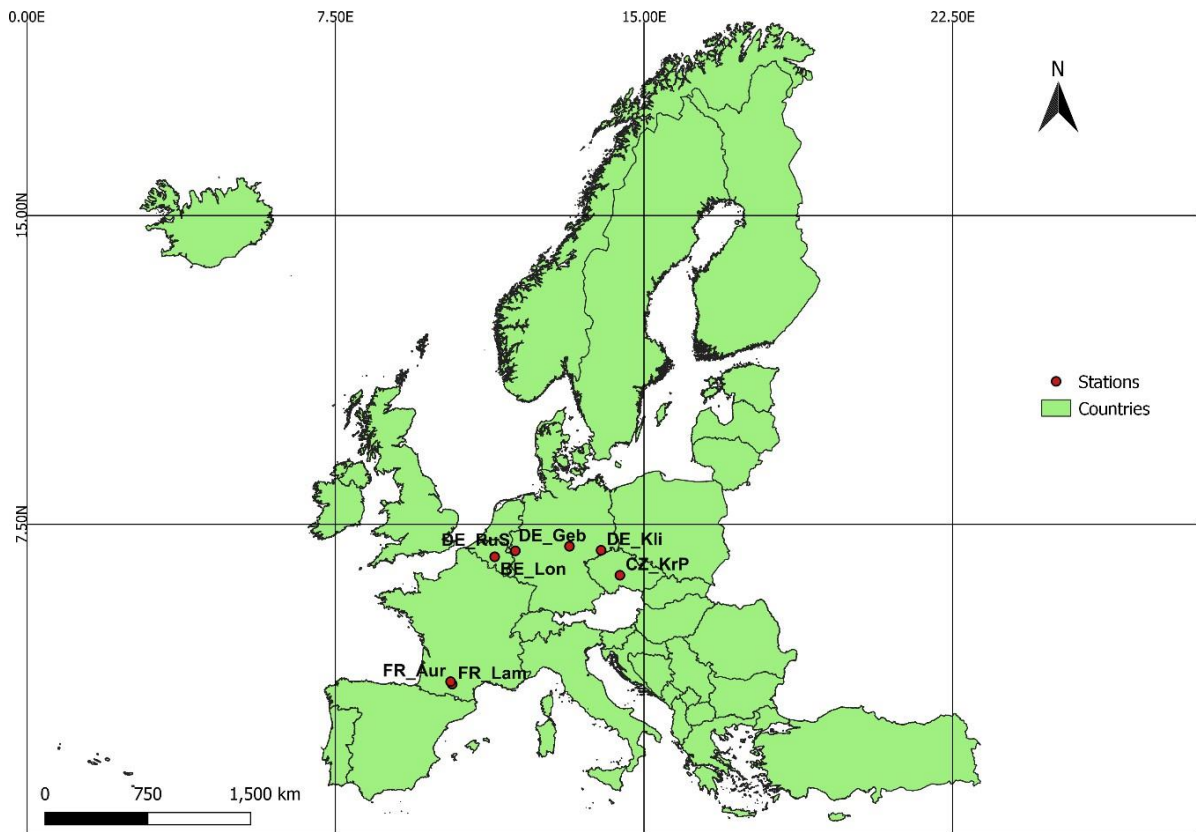


Figure 1. Study Area Map

#### 4. METHODOLOGY

This section outlines the methodology used to evaluate and compare the potential of WaPOR datasets for analysis. The workflow for dekadal data is shown in Figure 2, for seasonally aggregated data shown in Figure 3.

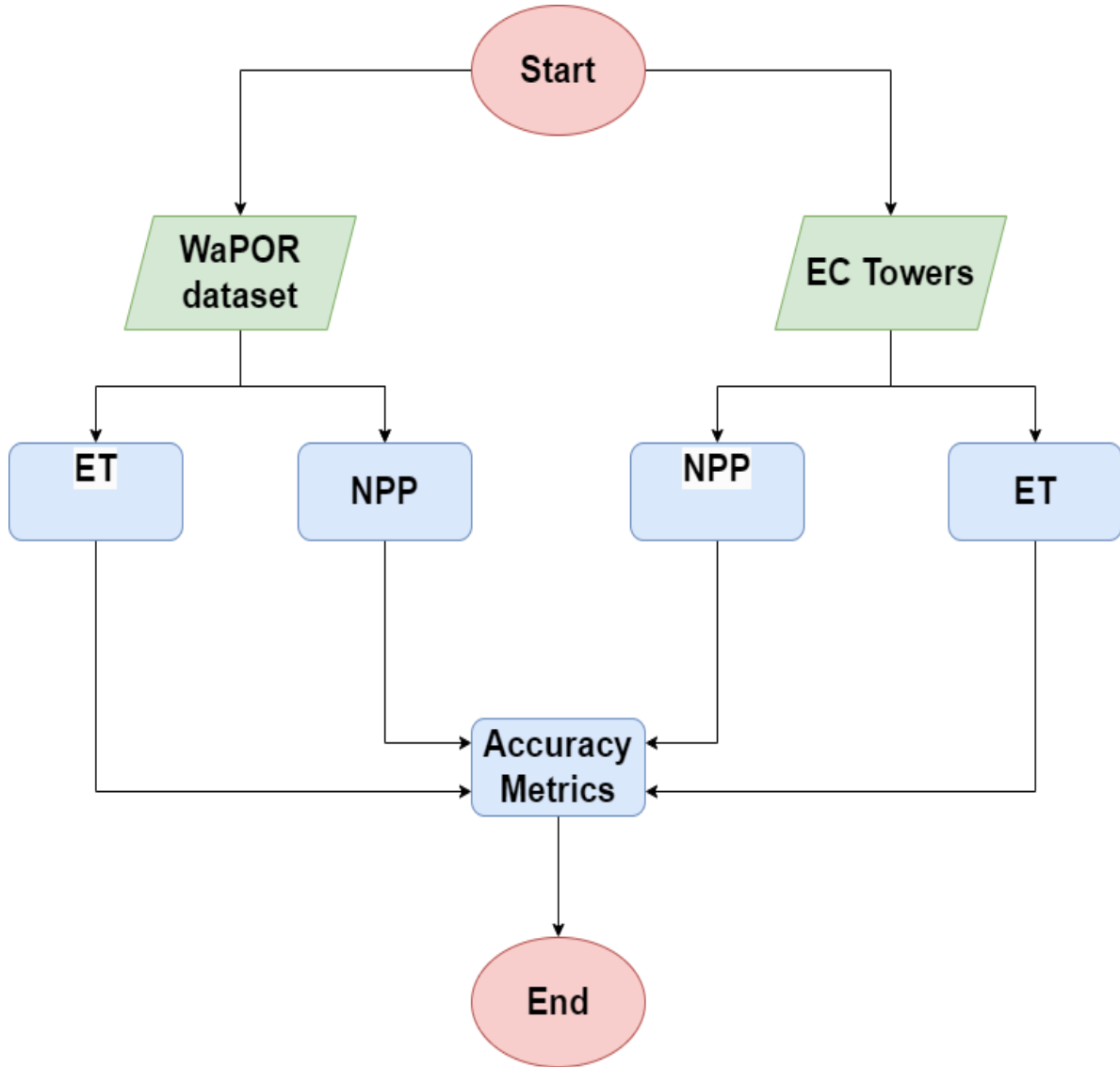


Figure 2 Dekadal data workflow

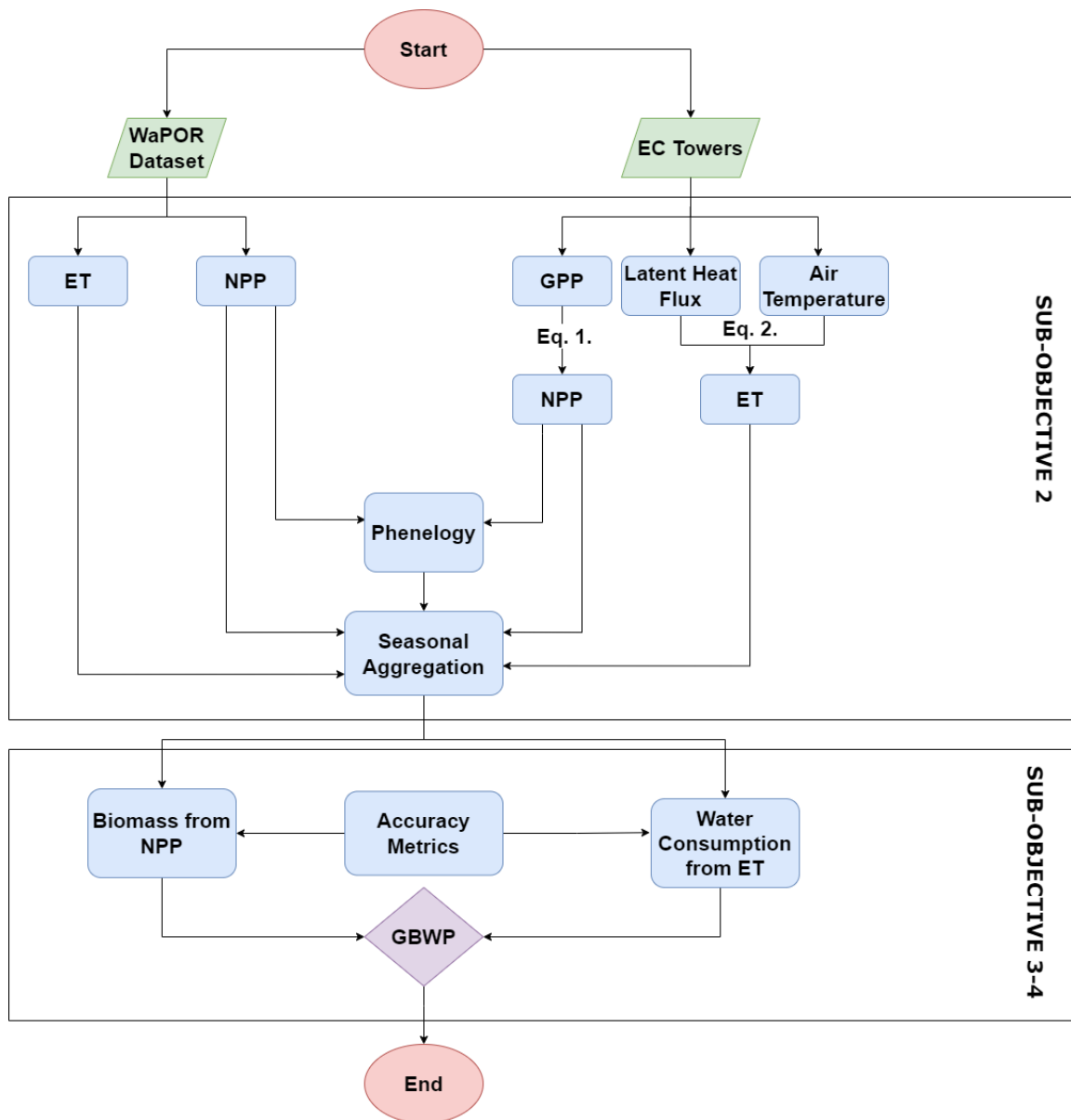


Figure 3. Seasonal value workflow

#### 4.1 Eddy Covariance Method

The eddy covariance method computes net ecosystem exchange (NEE) and fluxes of latent and sensible heat flux and momentum by co-varying high-frequency (10-20 times per second) measurements of concentrations of CO<sub>2</sub> and water and air temperature with the vertical component of the wind speed. An ecosystem may be as either source or absorber of CO<sub>2</sub> in the atmosphere, depending on whether photosynthesis or respiration is prevailing. This exchange of CO<sub>2</sub> between an ecosystem and the atmosphere is commonly considered as the net ecosystem exchange (NEE) and measured by eddy covariance tower (Baldocchi, 2003; Eugster & Merbold, 2015). Information obtained from the eddy covariance tower offers valuable metrics for ecosystem health and performance. It allows us to know the mass balance of vegetation and soils, as well as how the physiological dynamics of ecosystems react to environmental challenges (Baldocchi, 2014).

However, GPP and ET are not measured directly by EC towers (Álvarez-Taboada et al., 2015). Therefore, some processes have to be applied to obtain these data. Firstly, Net Ecosystem Exchange (NEE), measuring from EC towers, is converted to GPP by using assumptions (Lasslop et al., 2009). The purpose of the assumptions is to separate NEE into GPP and ecosystem respiration (R<sub>eco</sub>). The GPP data used in this study was separated from NEE using the night-time partitioning method, in which nighttime NEE, representing respiration, is subtracted from total NEE measurements to isolate GPP during the day (Pastorello et al., 2020). This method was explained in more detail by (Reichstein et al., 2005). Finally, GPP was converted to NPP using the generally accepted ratio of 50% (Sierra et al., 2022) and then from μmol CO<sub>2</sub> m<sup>-2</sup> s<sup>-1</sup> to g C day<sup>-1</sup> for compatibility with the WaPOR dataset (Eq. 1).

$$g C day^{-1} = \mu mol CO_2 m^{-2} s^{-1} \times \text{Molar mass of carbon} \times \text{Seconds in a day} \times 0.5 \quad (\text{Eq. 1})$$

On the other hand, ET data were obtained using latent heat flux and air temperature, and were later converted to mm/day for compatibility with WaPOR ET data (Eq. 2).

$$ET = \frac{\lambda E}{2.501 - (2.361 \times 10^{-3})T} \times 10^6 \times \text{Second in a day} \quad (\text{Eq. 2})$$

Where

ET: Evapotranspiration

λE: Latent heat flux [W m<sup>-2</sup>]

T: Air temperature [ °C]

The eddy covariance tower daily data used in this study are described in detail below. The data was obtained from the data portal of the Integrated Carbon Observation System (ICOS) project (<https://www.icos-cp.eu/data-services/about-data-portal>). Additionally, description of dataset was done by (Pastorello et al., 2020)

- GPP\_NT\_VUT\_USTAR50: This data refers to Gross Primary Productivity (GPP) and indicates the 50th percentile (USTAR50) of the Variable USTAR Threshold (VUT) determined by the Night Time Partitioning Method (NT).
- LE\_CORR: This data stands for Latent Heat Flux corrected (CORR) using the Bowen Ratio method.
- TA\_F: This data indicates air temperature in degrees Celsius, gap-filled using Marginal Distribution Sampling, a statistical method fills in missing data by estimating values based on the patterns observed in the existing data for that specific variable.

## 4.2 WaPOR

The WaPOR dataset was created as part of the 'Using Remote Sensing in Support of Solutions to Reduce Agricultural Water Productivity Gaps' project, which is funded by the Dutch government. The FAO is leading the project along with partners IHE Delft, IWMI, and the FRAME consortium. The project's objectives are to track water productivity, define deficiencies, offer improvements, and support sustainable agricultural production. Remote sensing data is provided by the FRAME consortium, consisting of the WaterWatch Foundation, VITO, ITC and eLEAF. The WaPOR portal underwent two independent quality assessments by ITC and IHE Delft before being released in beta form in April 2017 (FAO and IHE Delft, 2019). The evolution of the WaPOR model includes Version 2.1 and the latest global-scale version, WaPOR v3 (<https://data.apps.fao.org/wapor/?lang=en>). The underlying model is called ETLook and its description is provided in <https://www.fao.org/aquastat/py-wapor/etlook.html> and in the following sections.

We used two WaPOR v3 dataset in this study

- Actual evapotranspiration and interception (Global – Dekadal - 300m): This dataset provides important information on actual water consumption and how much rainfall is intercepted by leaves before reaching the grounds.
- NPP (Global – Dekadal): NPP is an important feature of the ecosystem, representing the conversion of carbon dioxide into plant biomass through photosynthesis.

### 4.2.1 Actual Evapotranspiration and Interception (AETI)

Evapotranspiration (ET) is a process where liquid water from various sources, such as soil moisture, water intercepted by plants, surface water, etc., transforms into vapor and enters the atmosphere (Tanner, 2015). This exchange allows us to understand Earth's water cycle and climate system. Remote sensing plays a critical role in monitoring this phenomenon over large areas.

However, direct measurement of AETI by satellites is not possible, it is derived from other components of the surface energy balance. These components are calculated using physical variables observable from space. Consequently, numerous remote sensing algorithms have been developed to estimate AETI (FAO and IHE Delft, 2019). The WaPOR calculates E and T is based on ETLook model which uses Penman-Monteith method. The Penman-Monteith equation uses common weather measurements to predict rate of total evaporation (E), and transpiration (T). Estimating evaporation, transpiration, and interception involves several

data components. Solar radiation, weather data are needed daily. Soil moisture stress, NDVI, and surface albedo are every ten days (*WaPOR Database Methodology*, 2020). The formula for the ETLook model, which solves the Penman-Monteith equation into two versions for soil (Eq. 3) and for vegetation (Eq.4).

$$\lambda E = \frac{\Delta(R_{n,soil}-G) + p_a c_p \frac{(e_s - e_a)}{r_{a,soil}}}{\Delta + \gamma \left(1 + \frac{r_{s,soil}}{r_{a,soil}}\right)} \quad (\text{Eq. 3})$$

And

$$\lambda T = \frac{\Delta(R_{n,canopy}-G) + p_a c_p \frac{(e_s - e_a)}{r_{a,canopy}}}{\Delta + \gamma \left(1 + \frac{r_{s,canopy}}{r_{a,canopy}}\right)} \quad (\text{Eq. 4})$$

Where:

$\lambda$ : Latent heat of evaporation [ $\text{J kg}^{-1}$ ]

$E$ : Evaporation [ $\text{kg m}^{-2} \text{s}^{-1}$ ]

$T$ : Transpiration [ $\text{kg m}^{-2} \text{s}^{-1}$ ]

$R_n$ : Net radiation [ $\text{W m}^{-2}$ ]

$G$ : Soil heat flux [ $\text{W m}^{-2}$ ]

$p_a$ : Air density [ $\text{kg m}^{-3}$ ]

$c_p$ : Specific heat of dry air [ $\text{J kg}^{-1} \text{K}^{-1}$ ]

$e_a$ : Actual vapour pressure of the air [Pa]

$e_s$ : Actual vapour pressure [Pa] which is a function of the air temperature

$\Delta$ : Slope of the saturation vapour pressure vs. Temperature curve [ $\text{Pa K}^{-1}$ ]

$\Gamma$ : Psychrometric constant [ $\text{Pa K}^{-1}$ ]

$r_a$ : Aerodynamic resistance [ $\text{s m}^{-1}$ ]

$r_s$ : Bulk surface resistance [ $\text{s m}^{-1}$ ]

#### 4.2.2 Net Primary Productivity (NPP)

The importance of terrestrial net primary production (NPP) in ecosystem science has increased significantly. This is because NPP plays a vital role in the carbon cycles of terrestrial environments and the dynamics of ecosystems. NPP refers to the amount of carbon captured by plants through photosynthesis within a specific time period (Pan et al., 2014). Additionally, it represents the amount of carbon that terrestrial ecosystems sequester after the assimilation process through photosynthesis (gross primary production

(GPP)), taking into account the losses caused by autotrophic respiration (Clark et al., 2001)

Both ground based and satellite based NPP models can be used to assess net primary production. However, the application of ground-based models is not operable in all areas. Consequently, satellite-based estimates of terrestrial primary production provide a regular and consistent assessment across the broad temporal and spatial dimensions (Pan et al., 2014)

Satellite-based estimates, such as those from WaPOR, provide a powerful tool for assessing NPP across large areas. Net Primary Productivity is derived from remote sensing and meteorological data. A significant enhancement was the incorporation of biome-specific light use efficiencies (LUEs). WaPOR employs this enhanced methodology. Additionally, two further refinements were made based on a review of the method. These refinements include:

- A factor that reduces the impact of short-term water deficiencies on soil moisture stress.
- The application of light use efficiencies (LUEs) that are specific to the kind of natural vegetation and crops identified by WaPOR.

Estimating Net Primary Production (NPP) relies on the following key components: daily weather data, solar radiation, dekadal fAPAR, and soil moisture stress (WaPOR Database Methodology, 2020). The equation is given below (Eq. 5)

$$NPP = Sc \times Rs \times \varepsilon_p \times fAPAR \times SM \times \varepsilon_{lue} \times \varepsilon_T \times \varepsilon_{CO2} \times \varepsilon_{AR} \times [\varepsilon_{RES}] \quad (\text{Eq.5})$$

Where:

Sc: Scaling factor from DMP to NPP [-]

Rs: Total shortwave incoming radiation [GJ<sub>T</sub>/ha/day]

ε<sub>p</sub>: Fraction of PAR in total shortwave 0.48 [JP/JT]

fAPAR: PAR-fraction absorbed by green vegetation [JPA/JP]

SM: Soil moisture stress reduction factor

ε<sub>lue</sub>: Light use efficiency at optimum [kgDM/GJPA]

ε<sub>T</sub>: Normalized temperature effect [-]

ε<sub>CO2</sub>: Normalized CO<sub>2</sub> fertilization effect [-]

ε<sub>AR</sub>: Fraction kept after autotrophic respiration [-]

ε<sub>RES</sub>: Fraction kept after residual effects [-]

### 4.3 Phenology

The study of cyclical natural phenomena, known as phenology, can be effectively assessed using the Normalized Difference Vegetation Index (NDVI) or net primary productivity (NPP).

NDVI, derived from satellite imagery, serves as a valuable indicator for evaluating the health and growth of vegetation by analyzing the difference in absorption of red and near-infrared light.



NDVI Time Series Analysis involves monitoring the progression of the growing season by tracking changes in NDVI values over time. Similarly, time series analysis of NPP can be used to track changes in plant productivity and water use throughout the growing season.

While traditionally used for assessing vegetation health, in this study, a threshold method was employed for the NPP data product. Specifically, phenology will be determined based on NPP values reaching a certain threshold. The start of the growing season (SOS) will be identified when each data set rises above this threshold, and the end of the season (EOS) will be considered when each data set falls below it (Gessesse & Melesse, 2019). This approach is crucial for monitoring the onset of the growing season, assessing crop health, and studying phenological stages of various plant species.

A 10-window size smoothing technique was employed for the NPP datasets (both EC and WaPOR) before phenological metrics extraction. The window size of 10 means that values of 100 days (10 decadal periods) within the window were averaged. The choice of a window size of 10 was based on the several attempts. This approach is aligned with the temporal granularity of our data, allowing us to preserve the inherent patterns and fluctuations present in the original datasets while reducing noise.

We compared SOS and EOS derived from eddy-covariance and WaPOR NPP.

#### 4.4 Seasonal Aggregation

Understanding phenology, in conjunction with Net Primary Productivity (NPP), allows for determining Total Biomass Production (TBP). TBP is calculated by summing the NPP converted to Dry Matter Productivity (DMP) units (kgDM/ha) from the start of the season (SOS) to the end of the season (EOS) using a formula provided by FAO and IHE Delft, (2020a) (Eq. 6).

$$Biomass = \sum_{i=SOS}^{EOS} Nd \times DMP \quad (\text{Eq. 6})$$

DMP, which stands for dry biomass production, is expressed as 1 gC/m<sup>2</sup>/day (NPP) = 22.222 kgDM/ha/day (DMP) equivalence, derived from Net Primary Productivity (NPP). Additionally, "Nd" represents the number of days.

The aggregation of ET to seasonal water consumption was done in a similar manner.

Two sets of seasonally aggregated values were computed, on dates derived from the measured NPP flux, further referred to as "flux dates" and from WaPOR NPP, "wapor dates"

#### 4.5 Gross Biomass Water Productivity (GBWP) Calculation

The ratio of grain yield to crop water use, or water use efficiency, offers a quick way to determine whether the yield is restricted by water availability or by other factors and is calculated using the formula below (Eq. 7) (Angus & van Herwaarden, 2001):

$$GBWP = \frac{Biomass}{Water\ Consumption} \quad (\text{Eq. 7})$$

#### 4.6 Accuracy Assessment

Several comparison metrics will be used to comprehensively assess the reliability of WaPOR v3 net primary productivity and evapotranspiration for calculating GBWP. These evaluations ensure a comprehensive assessment of the WaPOR's predictive accuracy, providing a holistic understanding of its performance across key variables.

Correlation ( $r$ ), as defined by Eq. 8, measures the strength and direction of the linear relationship between two variables. It ranges between -1 to 1. A positive value indicates a positive correlation, meaning both variables increase proportionally. Conversely, a negative correlation indicates that as one variable increases, the other decreases proportionally.

$$r = \frac{n(\sum XY) - (\sum X)(\sum Y)}{\sqrt{[n\sum X^2(\sum X)^2][n\sum Y^2(\sum Y)^2]}} \quad (\text{Eq. 8})$$

Where

X= Observed (EC) values,

Y= Model (WaPOR) values.

Another metric used in this study is Root Mean Squared Error (RMSE), measuring the average magnitude of the error between observed and field values. As the RMSE value approaches zero, it shows a better fit. RMSE equation is given below (Eq. 9).

$$RMSE = \sqrt{\sum_{i=1}^N \frac{(X_i - Y_i)^2}{N}} \quad (\text{Eq. 9})$$

Where

X= Observed (EC) values,

Y= Model (WaPOR) values.

Normalized Root Mean Square Error (nRMSE) is a measure used to evaluate the accuracy of a model's predictions by comparing them to actual observed values. It is calculated by dividing the Root Mean Square Error (RMSE) by the range of observed values. The equation is given below (Eq. 10).

$$nRMSE = \frac{RMSE}{X_{max} - X_{min}} \quad (\text{Eq. 10})$$

Where

$X_{max}$  = the maximum value of the field variable,

$X_{min}$  = the minimum value of the field variable.

Bias is calculated by determining the mean difference between estimates and observed values for both NPP and ET (Eq. 11).

$$Bias = \frac{1}{n} \sum^n (Y - X) \quad (\text{Eq. 11})$$

Where

X= Observed (EC) values,  
Y= Model (WaPOR) values.

$n \quad i=1$

Percentage Bias Error (PBE) is a statistical measure used to evaluate the accuracy of a predictive model by expressing the average bias between predicted and observed values as a percentage of the mean observed values. A positive PBE indicates that the model, on average, overestimates the observed values, while a negative PBE indicates an underestimation. The equation is given below (Eq. 12).

$$PBE = \left( \frac{\text{Bias}}{\bar{X}} \right) \times 100 \quad (\text{Eq. 12})$$

Where

$\bar{X}$  = The mean of observed (actual) value.

The Nash-Sutcliffe Efficiency (NSE) is a statistical metric used to assess the predictive accuracy of a model by comparing its output to observed data. NSE values range from  $-\infty$  to 1 (Eq. 13).

$$NSE = 1 - \frac{\sum_i (X_i - Y_i)^2}{\sum_i (X_i - \bar{X})^2} \quad (\text{Eq. 13})$$

Where

X = Observed value,

Y = Model (WaPOR) value,

$\bar{X}$  = mean of the observed value.

Kling-Gupta Efficiency (KGE) evaluates the overall goodness-of-fit between simulated and observed values, considering three components: correlation, variability, and bias. Higher values of KGE indicate better agreement between simulated and observed values, with 1 representing a perfect match. KGE equation is given below (Eq. 14)

$$KGE = 1 - \sqrt{(r - 1)^2 + (\alpha - 1)^2 + (\beta - 1)^2} \quad (\text{Eq. 14})$$

Where

r = correlation coefficient,

$\alpha$  = term representing the variability of prediction errors ( $\alpha Y/\alpha X$ ),

$\beta$  = bias term.

These measurements collectively provide a detailed assessment of the model's performance, providing a robust framework for evaluating the agreement, correlation, and bias between the WaPOR v3 NPP and actual field efficiency.

## 5. RESULTS

The average nRMSE of Net Primary Productivity (NPP) values across seven stations was 18%, while the average nRMSE of Evapotranspiration (ET) values were 16%. Additionally, when comparing the Start of Season (SOS) and End of Season (EOS) from WaPOR data with measurements from EC towers, the R-squared values were found to be 0.27 and 0.01, respectively. The result of the study was detailed in the following section.

### 5.1 Dekadal Data

In this study, WaPOR v3 dataset with 10-day temporal resolution was compared and validated with measurements obtained from Eddy covariance towers. The 10-day resolution of the WaPOR dataset entails aggregating measurements taken within each 10-day period (*WaPOR Database Methodology, 2020*). For instance, if measurements are available on the 1st and 11th day of a month, the data collected from the 1st to the 10th day are averaged and attributed to the 1st day of the month. This method was applied to direct measurement to ensure the reliability of the comparison made.

#### 5.1.1 Pixel Position Uncertainty

In this study, Net Primary Productivity (NPP) and Evapotranspiration (ET) were downloaded for seven cropland areas in Europe at a spatial resolution of 300 meters. Each cropland area is larger than 300 meters, ensuring that each area was covered by multiple pixels in our dataset (Figures 4-10).

To validate the WaPOR measurements, we compared them with in-situ data collected from an eddy covariance (EC) tower located within one of the cropland areas. The EC tower footprint, approximately 250 meters in radius (Chu et al., 2021) closely matches the resolution of our remote sensing data, making it a suitable reference for our study.

There were no significant differences in the annual accumulated total biomass values between the pixels. This homogeneity in pixel values supports the reliability of using a single representative measurement point for each area.

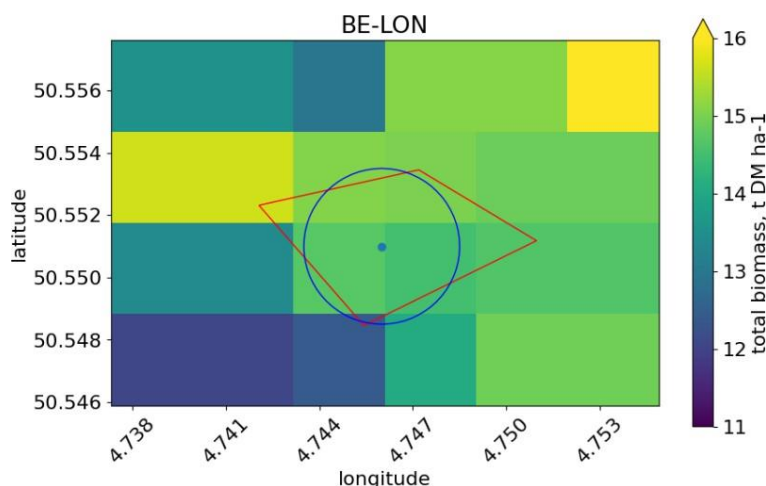


Figure 4. Pixel position map for BE\_Lon

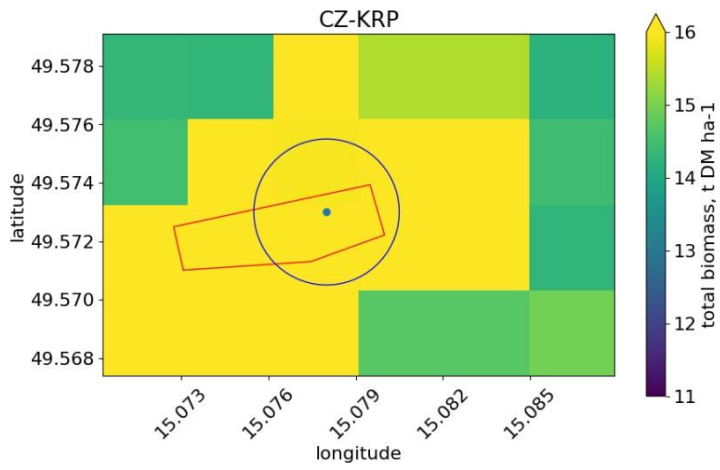


Figure 5. Pixel position map for CZ\_KrP

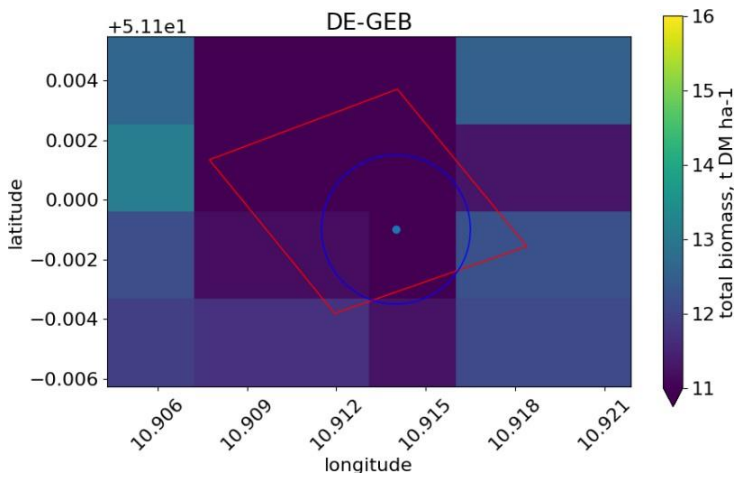


Figure 6. Pixel position map for DE\_Geb

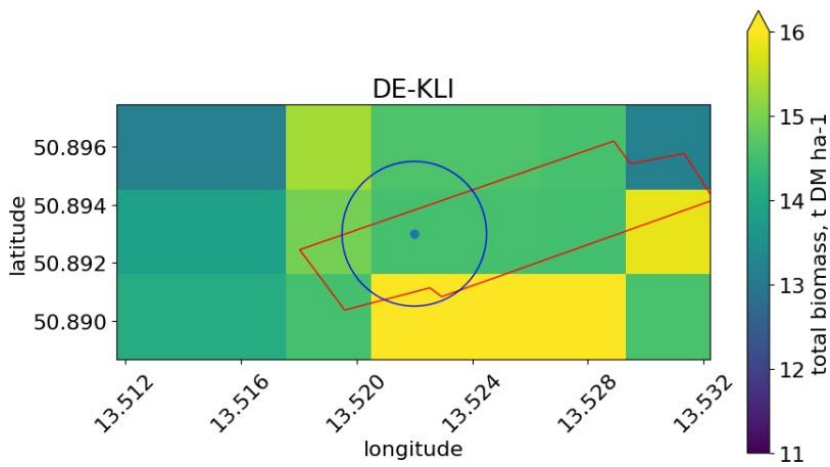


Figure 7. Pixel position map for DE\_Kli

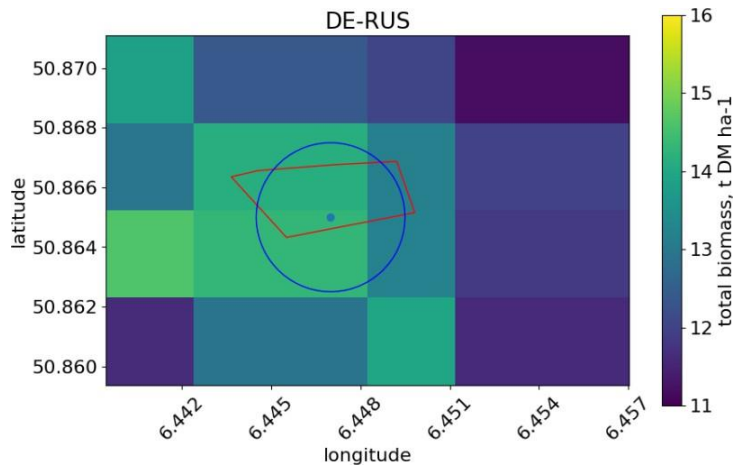


Figure 8. Pixel position map for DE\_Rus

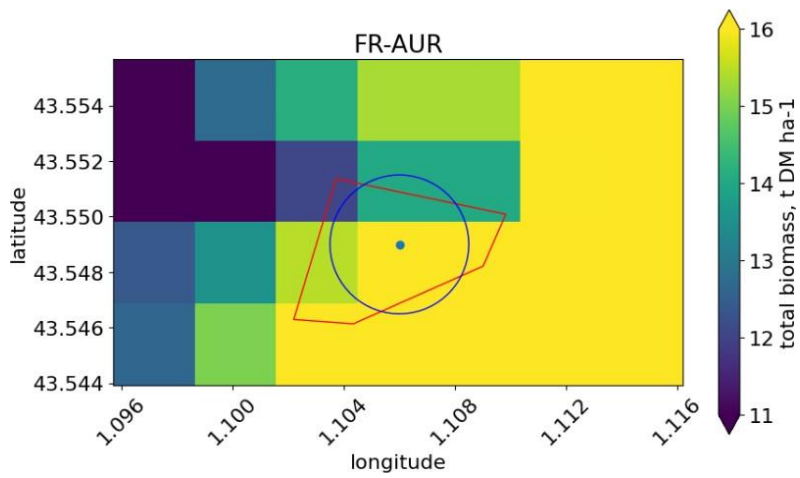


Figure 9. Pixel position map for FR\_Aur

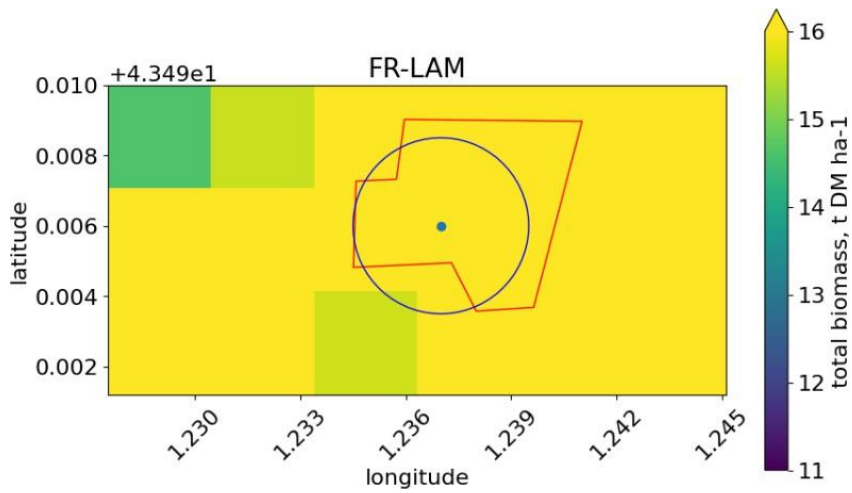


Figure 10. Pixel position map for FR\_Lam

### 5.1.2 Dekadal Patterns

Overall, WaPOR estimations show the same seasonal pattern as field measurements. However, deviations in values are observed. The WaPOR ET values (Figure 11, right) for the BE\_Lon station agree better with the observed values compared to the NPP (Figure 11, left), as indicated by the normalized Root Mean Square Error (nRMSE) values of 13% for ET and 16% for NPP. Among the seven observed fields, the nRMSE values of NPP for DE\_Kli (Figures 14), FR\_Lam (Figures 17), show higher consistency compared to the other stations with 11% and 14%, respectively. Additionally, the other German stations, DE\_Geb (Figure 13) and DE\_RuS (Figure 15), do not show a good fit for NPP, with nRMSE values of 18% and 22%. Due to WaPOR's overestimation in 2020, the FR\_Aur station has the worst nRMSE value for ET at 20%.

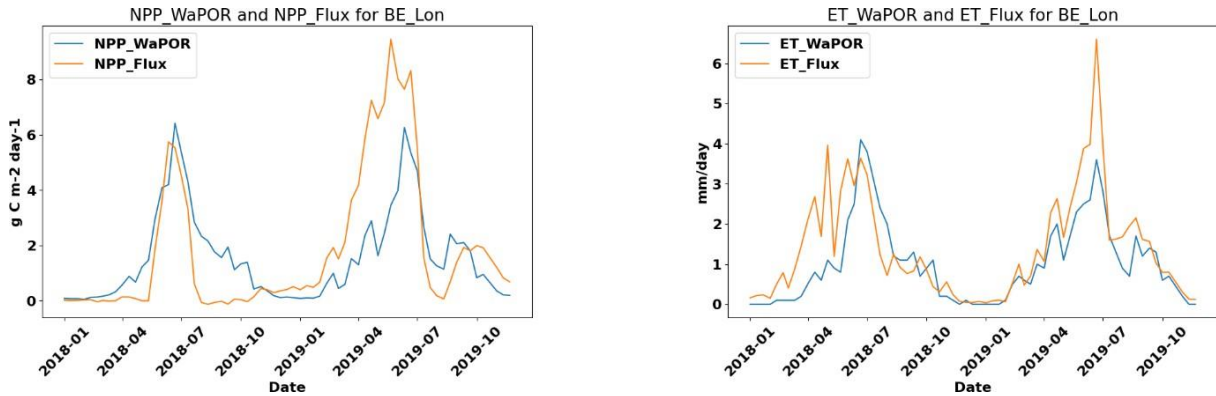


Figure 11. Comparison of NPP (left) and ET (right) between WaPOR and EC tower measurements for BE\_Lon

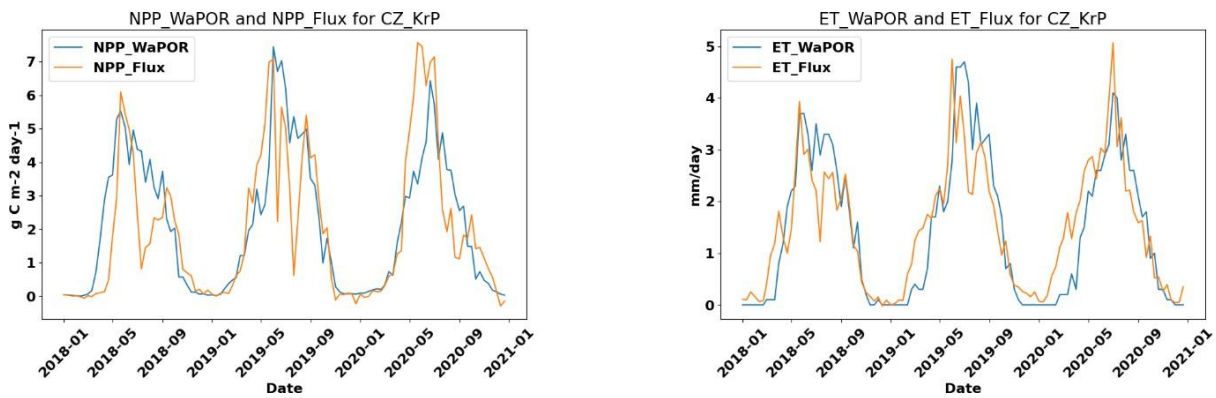


Figure 12. Comparison of NPP (left) and ET (right) between WaPOR and EC tower measurements for CZ\_KrP



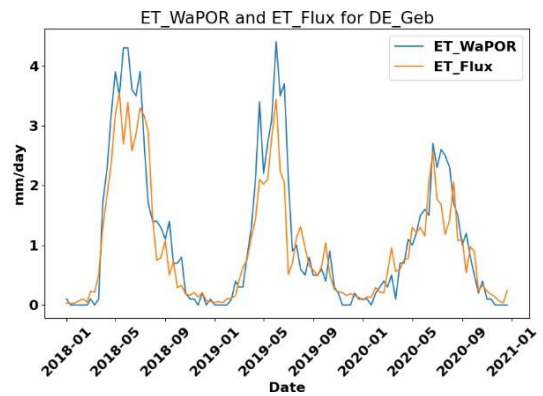
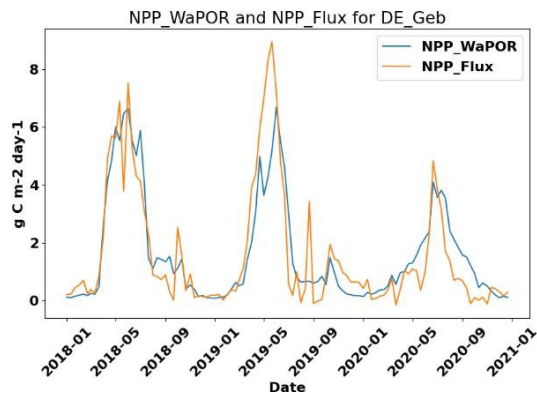


Figure 13. Comparison of NPP (left) and ET (right) between WaPOR and EC tower measurements for DE\_Geb

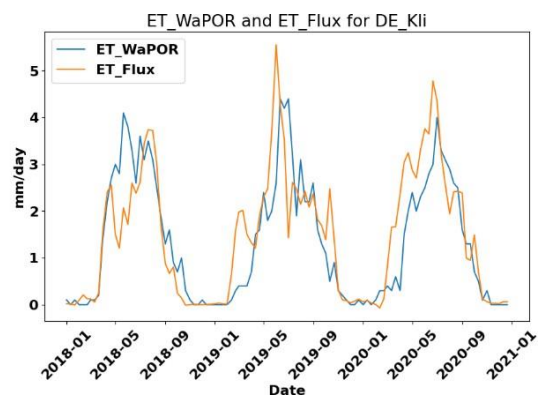
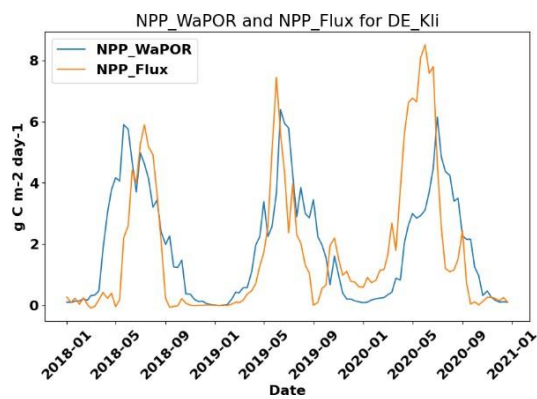


Figure 14. Comparison of NPP (left) and ET (right) between WaPOR and EC tower measurements for DE\_Kli

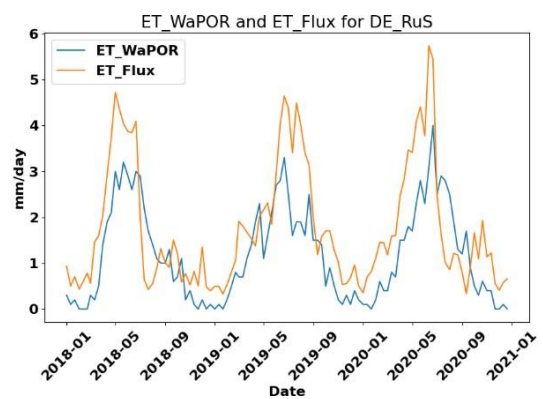
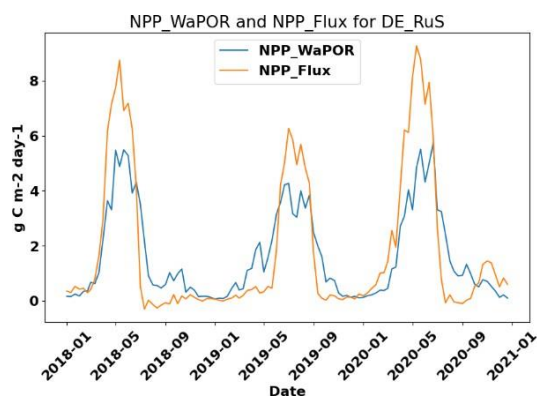


Figure 15. Comparison of NPP (left) and ET (right) between WaPOR and EC tower measurements for DE\_RuS

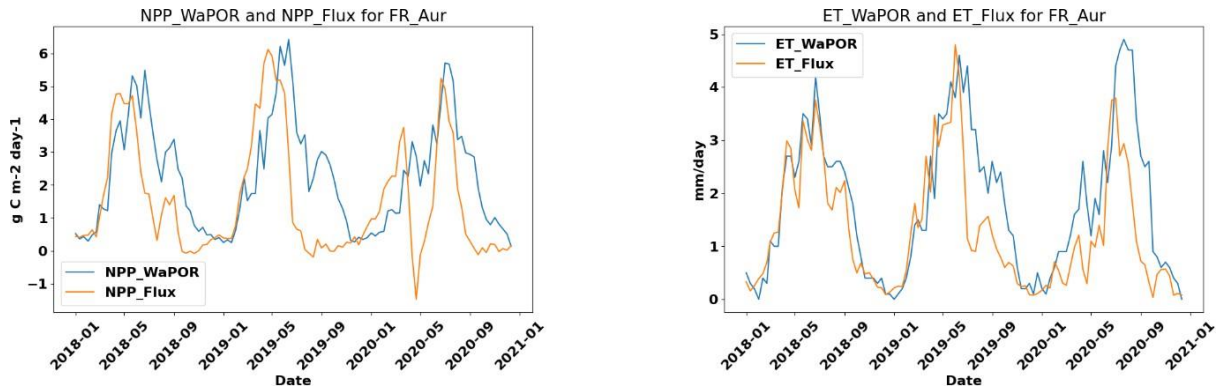


Figure 16. Comparison of NPP (left) and ET (right) between WaPOR and EC tower measurements for FR\_Aur

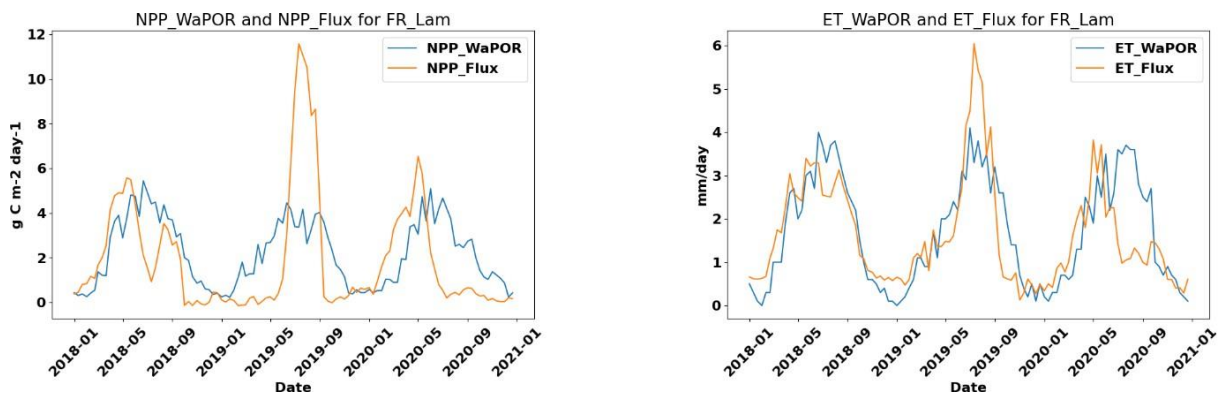


Figure 17. Comparison of NPP (left) and ET (right) between WaPOR and EC tower measurements for FR\_Lam

### 5.1.3 Special case: Station FR\_Aur

For the FR\_Aur station, the most notable issue is the shifted seasons between the WaPOR and field data. Another difference lies in the number of seasons. While four seasons were observed in the EC tower measurements between 2018 and 2020, the WaPOR estimation shows three seasons. Therefore, two separate external data sources were used for this station: NDVI values obtained from Sentinel-2 and data from field studies conducted by Ganeva et al., (2023). In Figure 18, which includes NDVI values, there is a high correlation between the EC towers and NDVI, both indicating four seasons. Ganeva's research findings confirm that there were four seasons between 2018 and 2020.

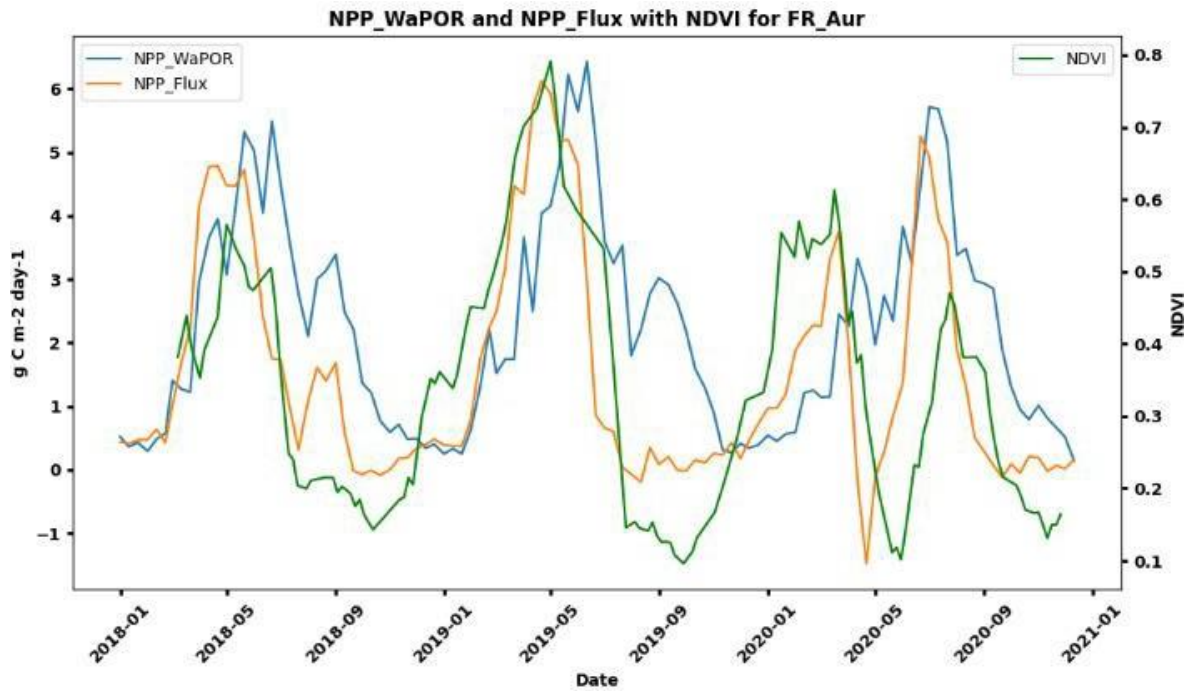


Figure 18. NPP WaPOR and NPP Flux with NDVI for FR\_Aur

### 5.1.4 Accuracy Metrics

The accuracy tests performed to assess the comparability between the WaPOR and field measurements are presented below. Table 2 shows the accuracy metrics for NPP. Table 3 provides the accuracy metrics for ET.

Table 2. Accuracy Metrics for NPP

Accuracy Metrics for NPP							
Station	RMSE [ g C m <sup>-2</sup> day <sup>-1</sup> ]	Bias [ g C m <sup>-2</sup> day <sup>-1</sup> ]	PBE	nRMSE	Correlation	NSE	KGE
BE_Lon	1.51	-0.23	-12%	16%	0.81	0.63	0.68
CZ_KrP	1.39	0.14	6%	18%	0.79	0.59	0.74
DE_Geb	1.02	0.02	1%	11%	0.87	0.76	0.80
DE_Kli	1.87	0.16	9%	22%	0.60	0.31	0.51
DE_RuS	1.46	-0.21	-11%	15%	0.88	0.70	0.65
FR_Aur	1.70	0.73	48%	22%	0.60	0.08	0.27
FR_Lam	2.31	0.28	15%	20%	0.49	0.22	0.27
<b>Average</b>	<b>1.6</b>	<b>0.13</b>	<b>8%</b>	<b>18%</b>	<b>0.72</b>	<b>0.47</b>	<b>0.56</b>

Overall, the RMSE of NPP is around 1.5 g C m<sup>-2</sup> day<sup>-1</sup>. With NPP values varying from 0.5 to 6 g C m<sup>-2</sup> day<sup>-1</sup>, the nRMSE results range from 11% to 23%. In addition, high correlation values obtained except for DE\_Kli and FR\_Aur and FR\_Lam stations are indicative of a

positive result. However, it is not possible to determine whether the WaPOR underestimates or overestimates NPP values over all sites when bias values are taken into account. The correlation value for NPP values was found to be 0.72 on average, indicating a medium-strong relationship with field measurements. It was also observed that the model slightly overestimated ( $0.13 \text{ g C m}^{-2} \text{ day}^{-1}$ ).

On the other hand, WaPOR demonstrated better performance in estimating ET with a lower RMSE of 0.83 mm/day. Additionally, the average KGE value was found to be 0.69, indicating acceptable performance with good correlation and acceptable bias. However, WaPOR slightly underestimated the ET values by  $-0.068 \text{ mm/day}$ .

Table 3. Accuracy Metrics for ET

Accuracy Metrics for ET							
Station	RMSE[mm/day]	Bias [mm/day]	PBE	nRMSE	Correlation	NSE	KGE
BE_Lon	0.859	-0.383	-27%	13%	0.811	0.571	0.662
CZ_KrP	0.705	-0.049	-3%	14%	0.868	0.654	0.741
DE_Geb	0.516	0.146	15%	14%	0.927	0.709	0.795
DE_Kli	0.838	-0.122	-8%	15%	0.809	0.619	0.782
DE_RuS	1.020	-0.590	-33%	19%	0.787	0.428	0.581
FR_Aur	0.962	0.470	35%	20%	0.791	0.308	0.564
FR_Lam	0.916	0.052	3%	15%	0.723	0.433	0.721
<b>Average</b>	<b>0.83</b>	<b>-0.068</b>	<b>-1.87%</b>	<b>16%</b>	<b>0.817</b>	<b>0.532</b>	<b>0.692</b>

## 5.2 Seasonal Aggregation

In this study, the threshold method based on an empirical approach was used to determine SOS and EOS (see Appendix A for dekadal patterns with threshold lines). NPP and water consumption values were aggregated in the determined seasons. It is detailed in the following sections.

### 5.2.1 Start of the season and end of the season uncertainty

SOS and EOS dates determined from smoothed Net Primary Productivity values are shown in the scatter plot Figure 19. According to the graph, the Start of Season (SOS) and End of Season (EOS) derived from WaPOR NPP values show poor agreement with those derived from field data. The SOS demonstrates slightly better alignment with an R-squared value of 0.27, while the R-squared value for EOS is extremely low at 0.01, indicating almost no correlation between WaPOR and field data. Generally, WaPOR predicts the start of the season 10 days earlier and the end of the season 66 days later compared to the field data, which is a significant discrepancy. This uncertainty may be attributed to factors such as the location of the fields, the specific years considered, and the types of crops planted.

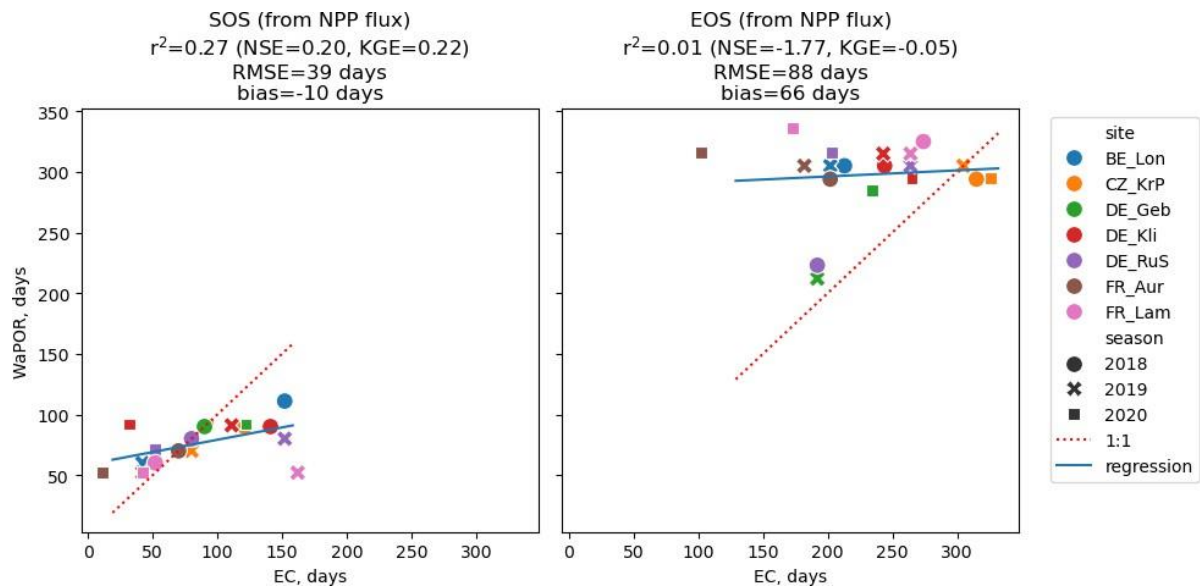


Figure 19. The start of the season (left) and end of the season (right) of NPP WaPOR and NPP Flux

However, Table 4, which shows the day difference between the WaPOR's SOS dates and the field data's SOS dates, provides a more detailed analysis. Negative values in the table indicate that WaPOR seasons start earlier than the field data. For instance, the first season at the BE\_Lon station starts 41 days later in the field data compared to the WaPOR data.

Table 4. The day difference for SOS between Flux and WaPOR

Day Difference for SOS in NPP							
	BE_Lon	CZ_KrP	DE_Geb	DE_Kli	DE_RuS	FR_Aur	FR_Lam
2018	41	-31	0	-51	0	0	8
2019	-18	-10	0	-20	-72	10	-110
2020		0	-30	60	19	41	10

On the other hand, when examining the end-of-season (EOS), larger date differences are observed compared to SOS, a phenomenon supported by Table 5. More positive values for EOS indicate that the WaPOR overestimated season endings compared to field data.

Table 5. The day difference for EOS between Flux and WaPOR

Day Difference for EOS in NPP							
	BE_Lon	CZ_KrP	DE_Geb	DE_Kli	DE_RuS	FR_Aur	FR_Lam
Season 1st	92	-21	61	61	31	92	51
Season 2nd	103	0	20	72	41	123	51
Season 3rd		-31	51	30	113	214	163

## 5.2.2 Total biomass

The scatter plots of Total Biomass (TB) values obtained by summing the NPP values over the season and then multiplying by the DMP constant and the number of days in the decade are provided below. (Figure 20). Three different scenarios were applied for Total biomass, water consumption, and GBWP: i) WaPOR and Flux values aggregated with Flux season dates, ii) WaPOR and Flux values aggregated with WaPOR dates, and iii) WaPOR and Flux values aggregated with their respective season dates. For a proper evaluation of the WaPOR, the comparison of both values within their respective dates should be considered. The other two scenarios were made to separate the uncertainty sources of dates and values.

The left graph, based on EC dates, demonstrates better performance with a moderate correlation and higher R-square value ( $r^2=0.39$ ) compared to the right graph. However, the model underestimates biomass when using EC dates, as indicated by a negative bias ( $-1.45 \text{ t DM ha}^{-1} \text{ season}^{-1}$ ), while WaPOR overestimates biomass when using WaPOR dates, shown by a positive bias ( $1.34 \text{ t DM ha}^{-1} \text{ season}^{-1}$ ). Despite these differences in bias direction, the root mean square error (RMSE) and bias as a percentage are relatively similar between the two scenarios.

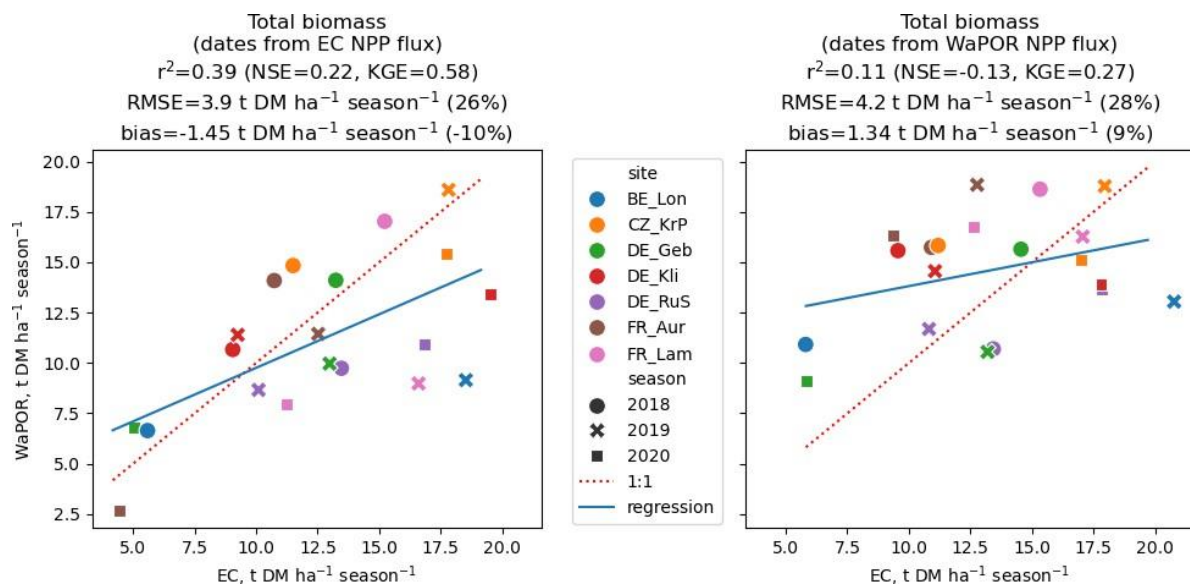


Figure 20. Comparison of Total Biomass Distribution: EC Days (Left) vs. WaPOR Days (Right)

The scatter plot compares gross biomass estimates derived from respective NPP flux (Figure 21). This case combines both uncertainty sources: in the aggregation dates and in the values. The graph shows a low correlation between the two datasets, with an r-square value of 0.08, indicating weak agreement. The performance metrics include KGE of 0.18, suggesting poor model performance. The RMSE is  $4.9 \text{ t DM ha}^{-1} \text{ season}^{-1}$  (33%), reflecting the relatively high prediction error, and the bias is  $2.01 \text{ t DM ha}^{-1} \text{ season}^{-1}$  (13%), indicating that WaPOR generally overestimates biomass compared to EC.



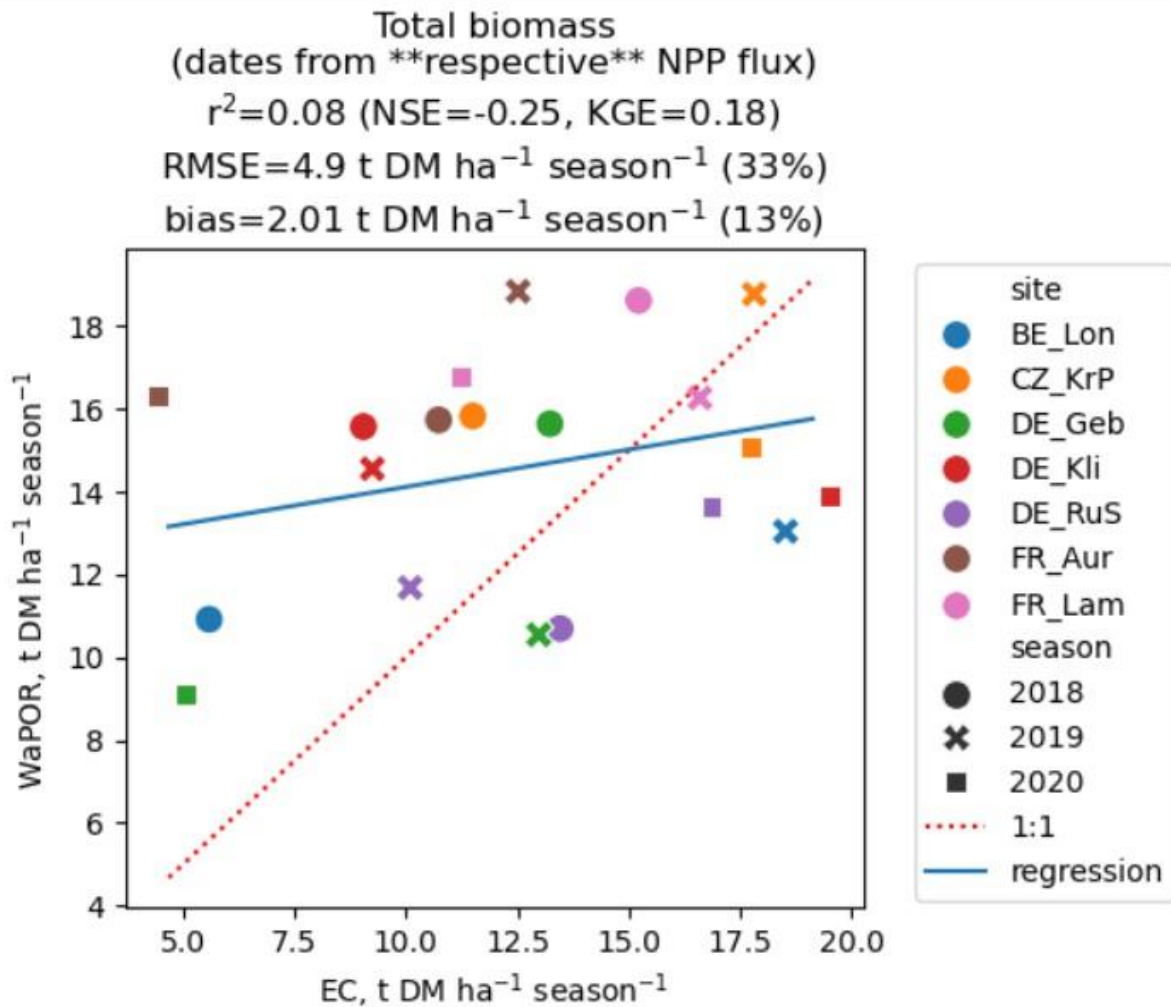


Figure 21. Comparison of Total Biomass with respective dates

### 5.2.3 Water consumption

The scatter plots representing water consumption values, which are the denominator for calculating Gross Biomass Water Productivity (GBWP), are given below (Figure 22). When aggregation was performed using the dates derived from the EC values the correlation was much stronger ( $r^2$  0.66) compared to the aggregation with WaPOR-derived dates ( $r^2$  0.17).

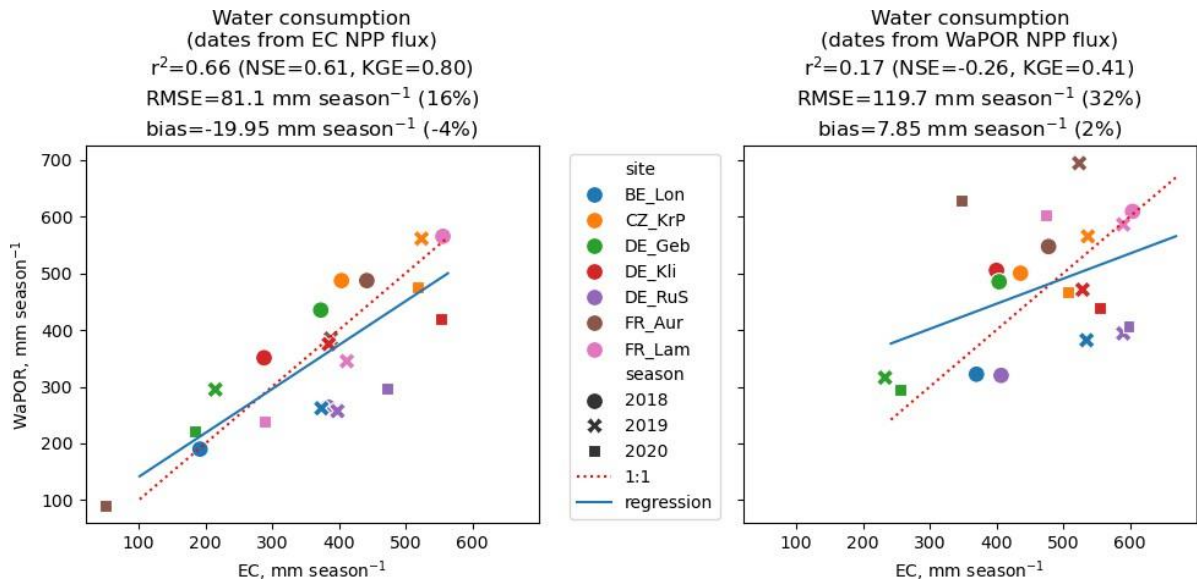


Figure 22. Distribution of WC values of WaPOR and Flux with EC days (Left) and WaPOR days (Right)

However, the weakest agreement is shown in the graph with the respective dates, where the correlation is very low (0.04) (Figure 23). The data points on the chart appear scattered randomly without any clear pattern. Additionally, in this scenario, the maximum RMSE value observed is 188.4 mm/season.

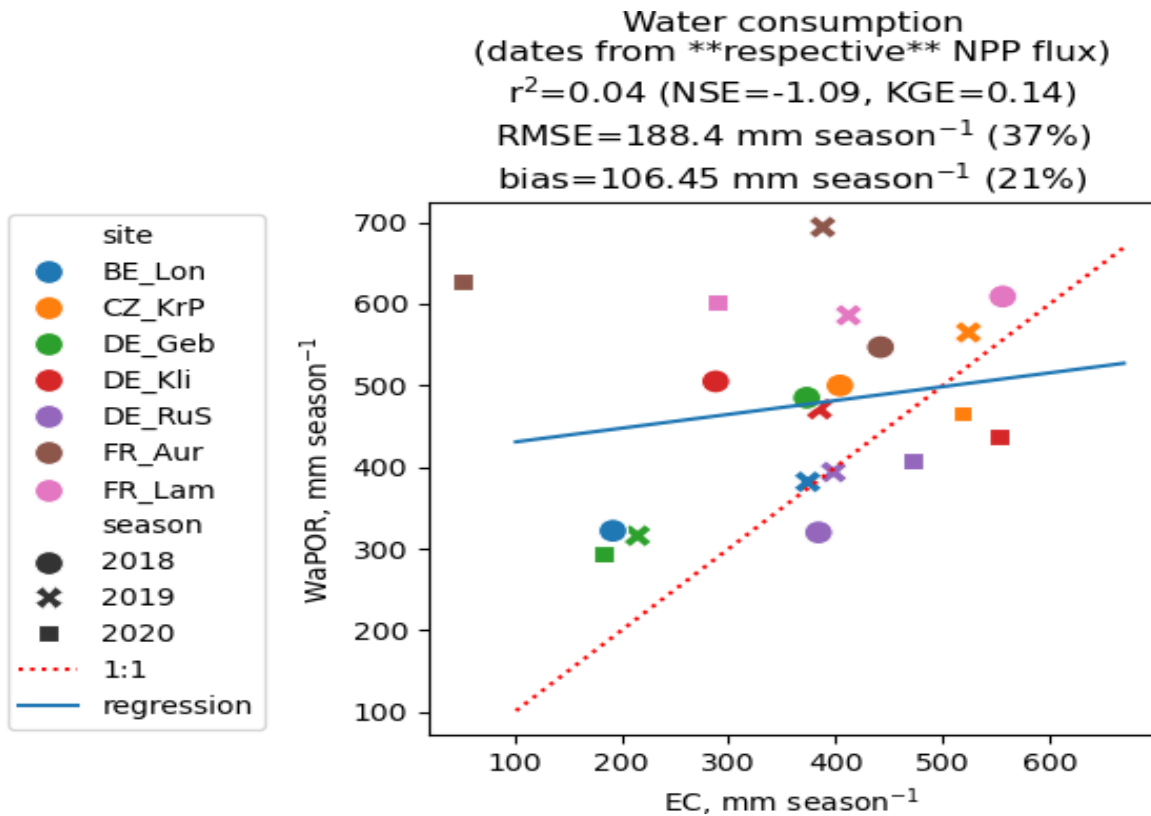


Figure 23. Distribution of WC values of WaPOR and Flux with Flux dates



### 5.3 Gross Biomass Water Productivity

The three graphs compare the Gross Biomass Water Productivity (GBWP) values obtained from WaPOR and Flux data, with each graph representing comparisons based on different dates. In these graphs, the horizontal axis represents the GBWP values measured by EC, while the vertical axis represents the GBWP values estimated by WaPOR.

On the right graph (Figure 24), the comparison based on WaPOR dates results in an  $R^2$  value of 0.16, indicating a weak linear relationship between the model and field data. The left graph (Figure 24), which compares data based on Flux dates, shows an even weaker correlation with an  $R^2$  value of 0.10. The graph evaluated with their respective dates (Figure 25) results in an  $R^2$  value of 0.1327, still indicating a weak relationship.

Overall, the three graphs collectively suggest that the WaPOR model does not consistently align with the Flux measurements across different dates and areas. The scatter of data points indicates that the WaPOR's predictions do not always match the field data and that discrepancies exist in certain areas.

Detailed comparisons for each station are provided in Table A.1-A.21 in the appendix.

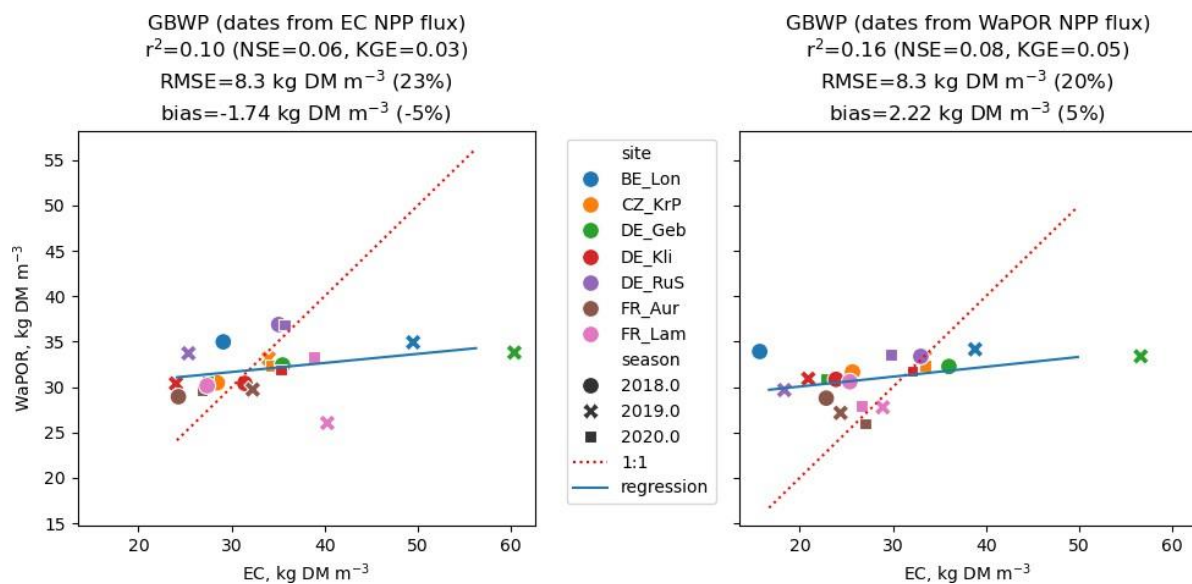


Figure 24. GBWP Flux vs WaPOR with EC towers dates (left) and WaPOR dates (right)

GBWP (dates from **\*\*respective\*\*** NPP flux)

$r^2=0.13$  (NSE=0.02, KGE=0.03)

RMSE=8.5 kg DM m<sup>-3</sup> (23%)

bias=-2.76 kg DM m<sup>-3</sup> (-8%)

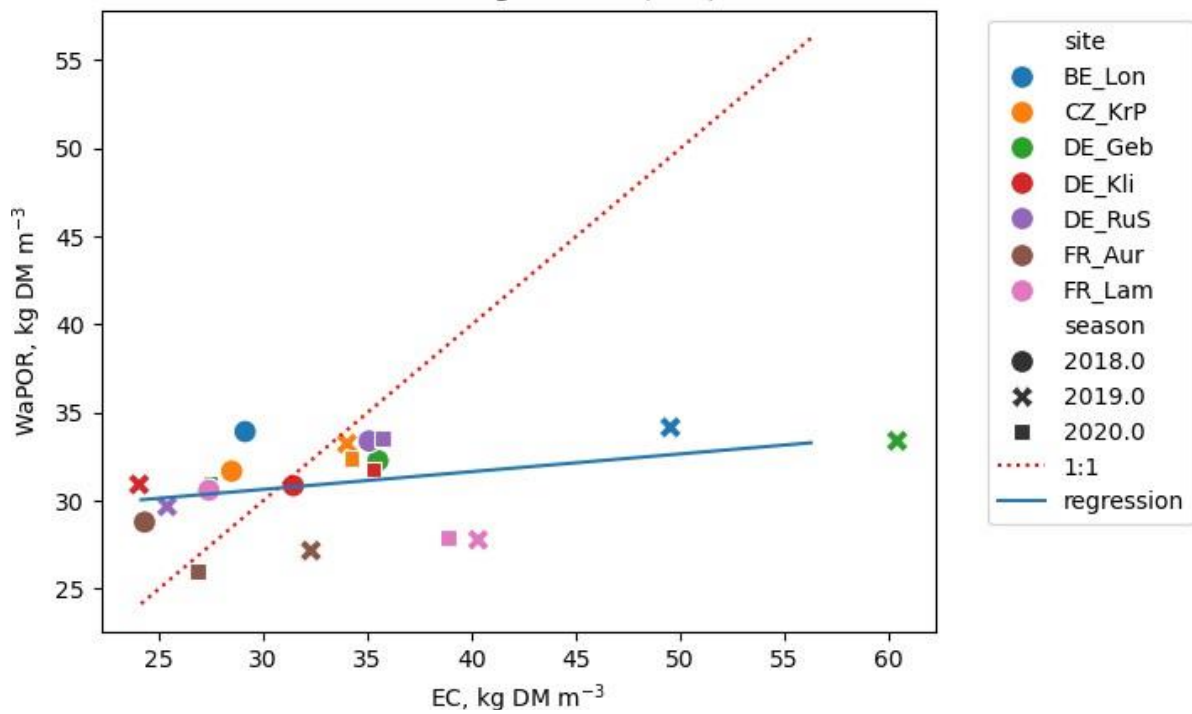


Figure 25. GBWP Flux vs WaPOR with respective dates

Overall, the RMSE and bias values are similar in all three graphs, indicating an underestimation of the model compared to field observations.

## 6. DISCUSSION

In this study, we evaluated the WaPOR v3 dataset for its effectiveness and reliability in estimating Net Primary Productivity (NPP) and evapotranspiration (ET) to calculate GBWP across multiple European sites. By comparing WaPOR v3 data with in-situ measurements, we aimed to determine the accuracy and applicability of WaPOR v3 for precision agriculture and water resource management. The findings highlight the potential of WaPOR v3 to provide accurate and useful data for agricultural planning while also revealing some limitations and areas for improvement.

In general, it can be said that the WaPOR model is comparable with field measurements of ET and NPP, and shows a consistent pattern in the dekadal graphs (Figure 11-17). The match of seasonally aggregated values depended on the flux. When aggregated based on EC-derived dates, water consumption showed a higher performance with an R-squared of 0.66 and an RMSE of 81.1 (16%) mm/season, compared to total biomass which showed an R-squared of 0.39 and an RMSE of 3.9 (26%) t DM ha<sup>-1</sup> season<sup>-1</sup>. Using WaPOR-derived dates to determine the season, water consumption had an R-squared of 0.17 and an RMSE of 32%, while total biomass had values of 0.11 and 28%, respectively. Lastly, when examined on their respective dates, water consumption achieved an R-squared of 0.04, whereas total biomass was 0.08. Overall, the WaPOR model demonstrated a higher ability to capture seasonal variations in water consumption compared to total biomass. Both variables performed best when aggregated using EC-derived dates. While the WaPOR model demonstrates strong performance in predicting ET (average correlation of 0.82) and NPP (correlation of 0.72), its ability to determine Start of Season (SOS) and End of Season (EOS) is notably weaker, as indicated by an R-squared value of 0.27 for SOS and only 0.01 for EOS. Several factors contribute to this uncertainty in accurately predicting the phenology such as climatic variability, crop rotation etc. As a result of these difficulties in accurately estimating SOS and EOS, there is less consistency in estimating water consumption, total biomass, and consequently, Gross Biomass Water Productivity (GBWP) values.

To better understand the performance of the WaPOR model, the accuracy metrics were compared with the performance of other models.

In a study by Zhu et al., (2016), the MODIS17A2 dataset's GPP product was evaluated across 8-day, and annual scales in China from 2003 to 2005. While the annual R-squared value of 0.76 indicated strong performance, the 8-day measurement yielded a lower R-squared value of 0.55. In contrast, in our study better performance was achieved on dekadal, rather than seasonal values. In our study, the average R-squared value was found to be 0.47. However, when excluding the special case of the FR\_Aur station, which showed an unusual difference, the R-squared value increases to 0.52. This indicates a slightly worse performance of WaPOR compared to MODIS17A2 at a similar temporal resolution.

Another evaluation by Ramoelo et al., (2014) in Skukuza, South Africa, from 2008 to 2010, investigated the MODIS17A2 ET product. This study reported RMSE values of 7.40, 7.39, and 4.30 mm/8-day and bias values of -9.43, -6.46, and 2.57 mm/8-day for ET measurements in 2008, 2009 and 2010, respectively. Considering the potentially higher range of ET values in the Skukuza study, comparison of PBias values between the two studies provides a more meaningful insight. PBias values in Skukuza vary between -16% and -51%, while WaPOR v3 PBias values range between -27% and 35%. In particular, stations CZ\_KrP, DE\_Kli, and FR\_Lam performed well, with PBias values of -3%, 8%, and 3%, respectively.

In a study conducted by Velpuri et al., (2013), the MOD16 and SSEBop datasets were evaluated between 2001 and 2007 in United States. The evaluation found R-squared values

of 0.7 for MOD16 and 0.66 for SSEBop from 50 observations in cropland areas. In our study, WaPOR v3 showed lower NSE values except for the DE\_Geb station. However, it is important to note that the RMSE values for MOD16 and SSEBop were relatively high, at 31 mm/month for MOD16 and 30 mm/month for SSEBop. Additionally, MOD16 and SSEBop underestimated ET values, with biases of -10 mm/month and -15 mm/month, respectively. In contrast, WaPOR v3 demonstrated better performance in terms of both RMSE and bias values, indicating a more accurate estimation of ET.

It is important to note that the time resolution of the data sets used in other compared studies was 8 days or months. In order to make a fair comparison, 8-day or monthly data must be converted to daily values. The high differences observed in RMSE and bias values may be due to not performing this transformation.

## **7. CONCLUSION**

In this study, the WaPOR v3 dataset was evaluated by comparing its values with field measurements. The study aimed to assess the alignment of WaPOR v3's NPP and AETI data with field observations, understand how uncertainty in SOS and EOS affects the consistency of seasonally aggregated values, and determine whether WaPOR v3 is adequate for calculating GBWP.

The comparison revealed that WaPOR v3 showed strong performance in predicting NPP and AETI, with average correlation coefficients of 0.72 and 0.82, respectively. The R-square value was found to be 0.47 for NPP and 0.53 for ET, indicating a moderate alignment of WaPOR v3 data with field observations. However, the model exhibited lower accuracy in predicting SOS and EOS, resulting in variability in the seasonal aggregation of data. These findings suggest that while WaPOR v3 is generally reliable for estimating key variables such as NPP and AETI, the identified uncertainties in SOS and EOS affect its performance. Therefore, the model's success in calculating GBWP is low and open to debate.

Future research should focus on validating WaPOR v3 across a wider range of ecosystem and climate conditions to ensure broader applicability of the findings. It is recommended to use external datasets to accurately identify seasons.

## Appendix A

### A.1 Dekadal Pattern for Phenology Retrieval

In the threshold method, 10% of the amplitude of the relevant data has been used, as seen in Equation A.1. Additionally, minor fluctuations in the graphs (Figure A 1-7) have been ignored when determining the start and end dates of the season.

$$\text{Threshold} = ((X_{\max} - X_{\min}) \times 0.1) + X_{\min} \quad (\text{Eq. A.1})$$

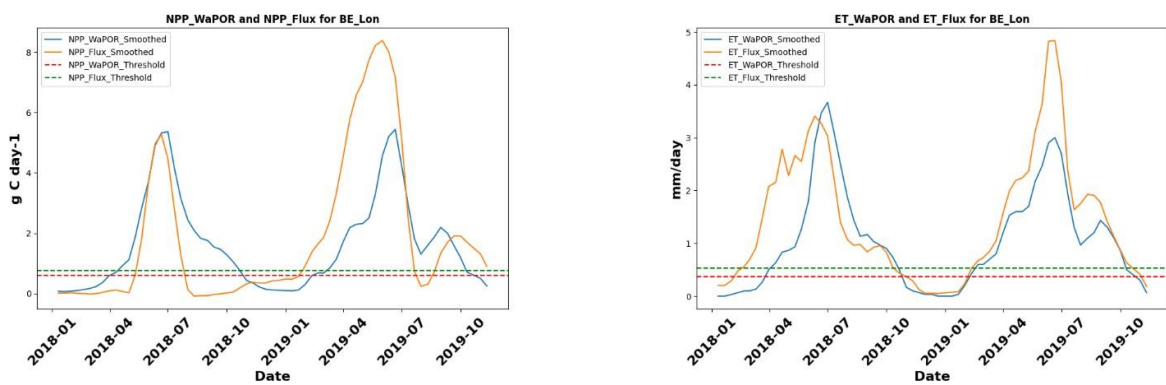


Figure A 1. Comparison of NPP (WaPOR vs. Flux) on the left and ET (WaPOR vs. Flux) on the right, with thresholds for BE\_Lon

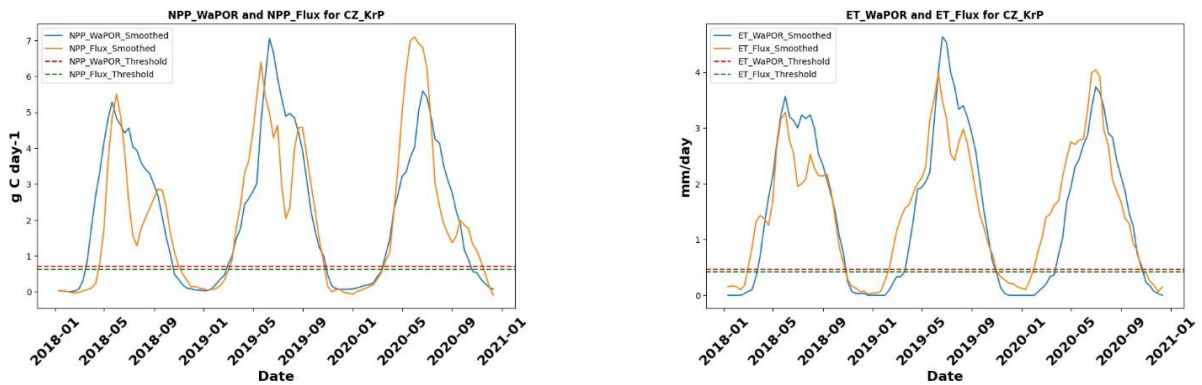


Figure A 2. Comparison of NPP (WaPOR vs. Flux) on the left and ET (WaPOR vs. Flux) on the right, with thresholds for CZ\_KrP

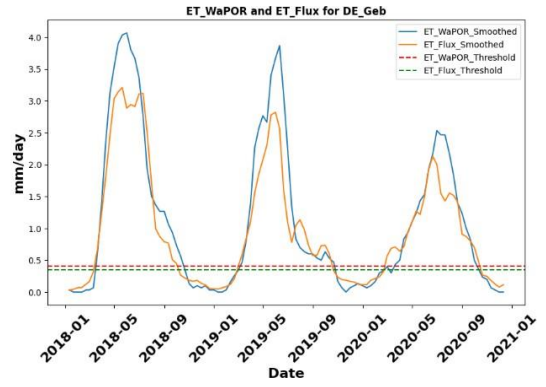
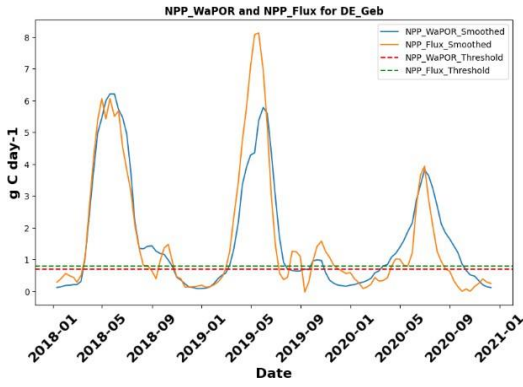


Figure A 3. Comparison of NPP (WaPOR vs. Flux) on the left and ET (WaPOR vs. Flux) on the right, with thresholds for DE\_Geb

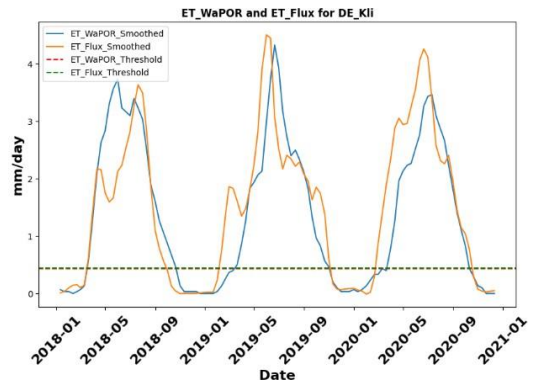
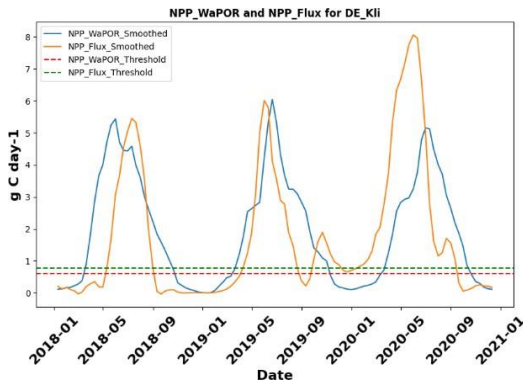


Figure A 4. Comparison of NPP (WaPOR vs. Flux) on the left and ET (WaPOR vs. Flux) on the right, with thresholds for DE\_Kli

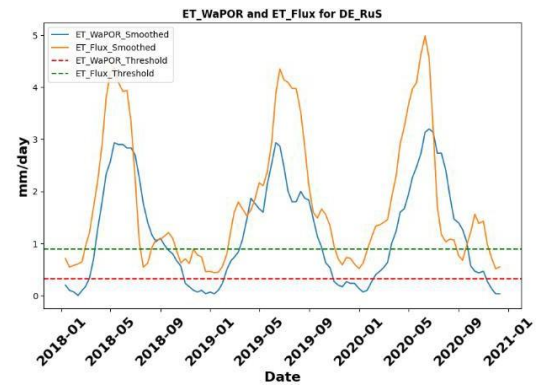
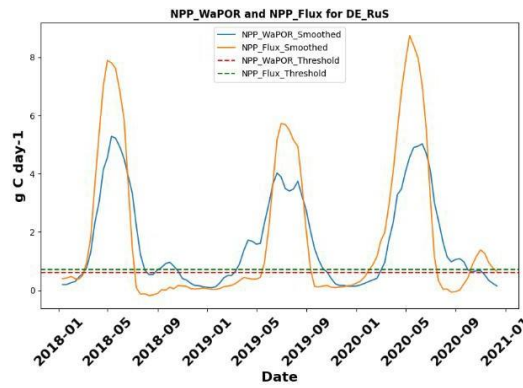


Figure A 5. Comparison of NPP (WaPOR vs. Flux) on the left and ET (WaPOR vs. Flux) on the right, with thresholds for DE\_RuS

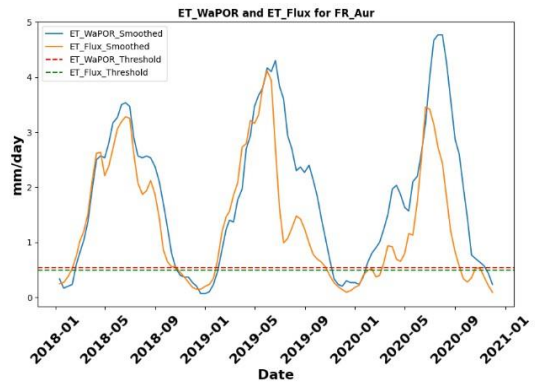
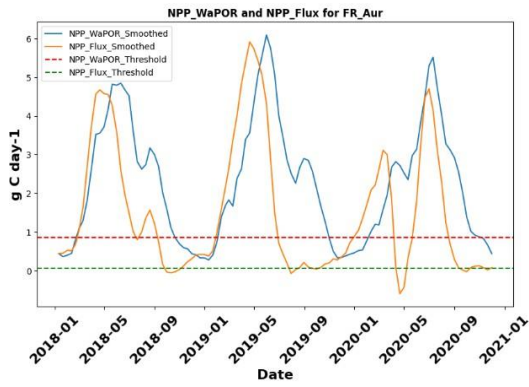


Figure A 6. Comparison of NPP (WaPOR vs. Flux) on the left and ET (WaPOR vs. Flux) on the right, with thresholds for FR\_Aur

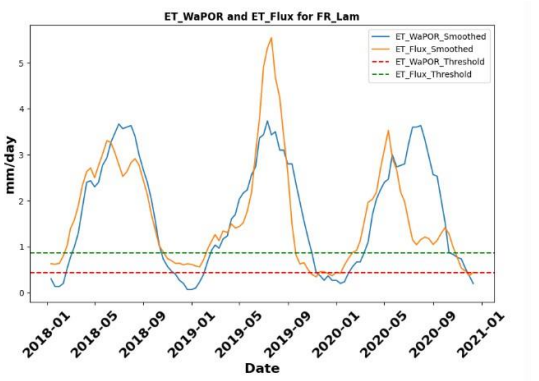
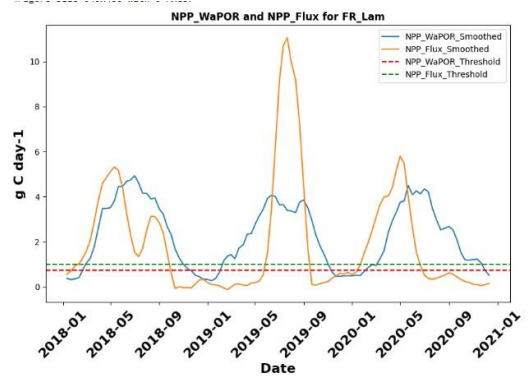


Figure A 7. Comparison of NPP (WaPOR vs. Flux) on the left and ET (WaPOR vs. Flux) on the right, with thresholds for FR\_Lam



## A.2 Gross Biomass Water Productivity

The results of the tables (Table A.1-21) created with GBWP values calculated using both field measurements and WaPOR data for each station do not show as much inconsistency as the results in the scatter plots in Figures 24, and 25. However, there is a disagreement both between stations and across different years.

Table A 1. GBWP values with Flux dates for BE\_Lon

<b>GBWP calculation (Flux dates) for BE_Lon</b>	Season 1st	Season 2nd
Biomass_WaPOR (kgDM/ha/season)	6645	9150
Biomass_Flux (kgDM/ha/season)	5589	18518
Water_Consumption_WaPOR (mm/season)	190	262
Water_Consumption_Flux (mm/season)	192	374
<b>GBWP_WaPOR (kgDM/m<sup>3</sup> H<sub>2</sub>O)</b>	<b>34.97</b>	<b>34.92</b>
<b>GBWP_Flux (kgDM/m<sup>3</sup> H<sub>2</sub>O)</b>	<b>29.11</b>	<b>49.51</b>

Table A 2. GBWP values with WaPOR dates for BE\_Lon

<b>GBWP calculation ( WaPOR dates) for BE_Lon</b>	Season 1st	Season 2nd
Biomass_WaPOR (kgDM/ha /season)	10919	13045
Biomass_Flux (kgDM/ha /season)	5805	20773
Water_Consumption_WaPOR (mm/season)	322	382
Water_Consumption_Flux (mm/season)	370	535
<b>GBWP_WaPOR (kgDM/m<sup>3</sup> H<sub>2</sub>O)</b>	<b>33.90</b>	<b>34.15</b>
<b>GBWP_Flux (kgDM/m<sup>3</sup> H<sub>2</sub>O)</b>	<b>15.69</b>	<b>38.82</b>

Table A 3. GBWP values with their respective dates for BE\_Lon

<b>GBWP calculation for BE_Lon</b>	Season 1st	Season 2nd
Biomass_WaPOR (kgDM/ha /season)	10919	13045
Biomass_Flux (kgDM/ha /season)	5589	18518
Water_Consumption_WaPOR (mm/season)	322	382
Water_Consumption_Flux (mm/season)	192	374
<b>GBWP_WaPOR (kgDM/m<sup>3</sup> H<sub>2</sub>O)</b>	<b>33.90</b>	<b>34.15</b>
<b>GBWP_Flux (kgDM/m<sup>3</sup> H<sub>2</sub>O)</b>	<b>29.11</b>	<b>49.5</b>

Table A 4 .GBWP values with Flux dates for CZ\_KrP

<b>GBWP calculation (Flux dates) for CZ_KrP</b>	Season 1st	Season 2nd	Season 3rd
Biomass_WaPOR (kgDM/ha /season)	14835	18591	15425
Biomass_Flux (kgDM/ha /season)	11502	17817	17724
Water_Consumption_WaPOR (mm/season)	487	561	476
Water_Consumption_Flux (mm/season)	404	524	518
<b>GBWP_WaPOR (kgDM/m<sup>3</sup> H<sub>2</sub>O)</b>	<b>30.46</b>	<b>33.14</b>	<b>32.41</b>
<b>GBWP_Flux (kgDM/m<sup>3</sup> H<sub>2</sub>O)</b>	<b>28.47</b>	<b>34.00</b>	<b>34.22</b>

Table A 5. GBWP values with WaPOR dates for CZ\_KrP

<b>GBWP calculation ( WaPOR dates) for CZ_KrP</b>	Season 1st	Season 2nd	Season 3rd
Biomass_WaPOR (kgDM/ha /season)	15830	18775	15105
Biomass_Flux (kgDM/ha /season)	11187	17956	16989
Water_Consumption_WaPOR (mm/season)	500	565	466
Water_Consumption_Flux (mm/season)	436	537	507
<b>GBWP_WaPOR (kgDM/m<sup>3</sup> H<sub>2</sub>O)</b>	<b>31.66</b>	<b>33.23</b>	<b>32.42</b>
<b>GBWP_Flux (kgDM/m<sup>3</sup> H<sub>2</sub>O)</b>	<b>25.66</b>	<b>33.44</b>	<b>33.51</b>

Table A 6 .GBWP values with their respective for CZ\_KrP

<b>GBWP calculation for CZ_KrP</b>	Season 1st	Season 2nd	Season 3rd
Biomass_WaPOR (kgDM/ha /season)	15830	18775	15105
Biomass_Flux (kgDM/ha /season)	11502	17817	17724
Water_Consumption_WaPOR (mm/season)	500	565	466
Water_Consumption_Flux (mm/season)	404	524	518
<b>GBWP_WaPOR (kgDM/m<sup>3</sup> H<sub>2</sub>O)</b>	<b>31.66</b>	<b>33.23</b>	<b>32.42</b>
<b>GBWP_Flux (kgDM/m<sup>3</sup> H<sub>2</sub>O)</b>	<b>28.47</b>	<b>34.00</b>	<b>34.22</b>

Table A 7.GBWP values with Flux dates for DE\_Geb

<b>GBWP calculation (Flux dates) for DE_Geb</b>	Season 1st	Season 2nd	Season 3rd
Biomass_WaPOR (kgDM/ha /season)	14103	9969	6783
Biomass_Flux (kgDM/ha /season)	13236	12984	5050
Water_Consumption_WaPOR (mm/season)	435	295	222
Water_Consumption_Flux (mm/season)	373	215	184
<b>GBWP_WaPOR (kgDM/m<sup>3</sup> H<sub>2</sub>O)</b>	<b>32.42</b>	<b>33.79</b>	<b>30.56</b>
<b>GBWP_Flux (kgDM/m<sup>3</sup> H<sub>2</sub>O)</b>	<b>35.49</b>	<b>60.39</b>	<b>27.45</b>

Table A 8.GBWP values with WaPOR dates for DE\_Geb

<b>GBWP calculation ( WaPOR dates) for DE_Geb</b>	Season 1st	Season 2nd	Season 3rd
Biomass_WaPOR (kgDM/ha /season)	15644	10549	9099
Biomass_Flux (kgDM/ha /season)	14552	13194	5843
Water_Consumption_WaPOR (mm/season)	485	316	294
Water_Consumption_Flux (mm/season)	404	233	256
<b>GBWP_WaPOR (kgDM/m<sup>3</sup> H<sub>2</sub>O)</b>	<b>32.26</b>	<b>33.38</b>	<b>30.95</b>
<b>GBWP_Flux (kgDM/m<sup>3</sup> H<sub>2</sub>O)</b>	<b>36.02</b>	<b>56.63</b>	<b>22.83</b>

Table A 9.GBWP values with their respective for DE\_Geb

<b>GBWP calculation for DE_Geb</b>	Season 1st	Season 2nd	Season 3rd
Biomass_WaPOR (kgDM/ha /season)	15644	10549	9099
Biomass_Flux (kgDM/ha /season)	13236	12984	5050
Water_Consumption_WaPOR (mm/season)	485	316	294
Water_Consumption_Flux (mm/season)	404	233	256
<b>GBWP_WaPOR (kgDM/m<sup>3</sup> H<sub>2</sub>O)</b>	<b>32.26</b>	<b>33.38</b>	<b>30.95</b>
<b>GBWP_Flux (kgDM/m<sup>3</sup> H<sub>2</sub>O)</b>	<b>32.76</b>	<b>55.73</b>	<b>19.73</b>

Table A 10. GBWP values with Flux dates for DE\_Kli

<b>GBWP calculation (Flux dates) for DE_Kli</b>	Season 1st	Season 2nd	Season 3rd
Biomass_WaPOR (kgDM/ha /season)	10670	11395	13394
Biomass_Flux (kgDM/ha /season)	9051	9251	19504
Water_Consumption_WaPOR (mm/season)	351	375	420
Water_Consumption_Flux (mm/season)	288	385	553
<b>GBWP_WaPOR (kgDM/m<sup>3</sup> H<sub>2</sub>O)</b>	<b>30.40</b>	<b>30.39</b>	<b>31.89</b>
<b>GBWP_Flux (kgDM/m<sup>3</sup> H<sub>2</sub>O)</b>	<b>31.43</b>	<b>24.03</b>	<b>35.27</b>

Table A 11. GBWP values with WaPOR dates for DE\_Kli

<b>GBWP calculation ( WaPOR dates) for DE_Kli</b>	Season 1st	Season 2nd	Season 3rd
Biomass_WaPOR (kgDM/ha /season)	15574	14557	13910
Biomass_Flux (kgDM/ha /season)	9554	11060	17809
Water_Consumption_WaPOR (mm/season)	505	471	438
Water_Consumption_Flux (mm/season)	400	529	555
<b>GBWP_WaPOR (kgDM/m<sup>3</sup> H<sub>2</sub>O)</b>	<b>30.84</b>	<b>30.91</b>	<b>31.76</b>
<b>GBWP_Flux (kgDM/m<sup>3</sup> H<sub>2</sub>O)</b>	<b>23.89</b>	<b>20.91</b>	<b>32.09</b>

Table A 12. GBWP values with respective dates for DE\_Kli

<b>GBWP calculation for DE_Kli</b>	Season 1st	Season 2nd	Season 3rd
Biomass_WaPOR (kgDM/ha /season)	15574	14557	13910
Biomass_Flux (kgDM/ha /season)	9051	9251	19504
Water_Consumption_WaPOR (mm/season)	505	471	438
Water_Consumption_Flux (mm/season)	400	529	555
<b>GBWP_WaPOR (kgDM/m<sup>3</sup> H<sub>2</sub>O)</b>	<b>30.84</b>	<b>30.91</b>	<b>31.76</b>
<b>GBWP_Flux (kgDM/m<sup>3</sup> H<sub>2</sub>O)</b>	<b>22.63</b>	<b>17.49</b>	<b>35.14</b>

Table A 13. GBWP values with Flux dates for DE\_RuS

<b>GBWP calculation (Flux dates) for DE_RuS</b>	Season 1st	Season 2nd	Season 3rd
Biomass_WaPOR (kgDM/ha /season)	9737	8664	10949
Biomass_Flux (kgDM/ha /season)	13464	10098	16851
Water_Consumption_WaPOR (mm/season)	264	257	297
Water_Consumption_Flux (mm/season)	384	398	472
<b>GBWP_WaPOR (kgDM/m<sup>3</sup> H<sub>2</sub>O)</b>	<b>36.88</b>	<b>33.71</b>	<b>36.87</b>
<b>GBWP_Flux (kgDM/m<sup>3</sup> H<sub>2</sub>O)</b>	<b>35.06</b>	<b>25.37</b>	<b>35.70</b>

Table A 14. GBWP values with WaPOR dates for DE\_RuS

<b>GBWP calculation ( WaPOR dates) for DE_RuS</b>	Season 1st	Season 2nd	Season 3rd
Biomass_WaPOR (kgDM/ha /season)	10697	11687	13650
Biomass_Flux (kgDM/ha /season)	13428	10816	17827
Water_Consumption_WaPOR (mm/season)	320	394	407
Water_Consumption_Flux (mm/season)	407	590	598
<b>GBWP_WaPOR (kgDM/m<sup>3</sup> H<sub>2</sub>O)</b>	<b>33.37</b>	<b>29.66</b>	<b>33.54</b>
<b>GBWP_Flux (kgDM/m<sup>3</sup> H<sub>2</sub>O)</b>	<b>32.99</b>	<b>18.33</b>	<b>29.81</b>

Table A 15. GBWP values with respective dates for DE\_RuS

<b>GBWP calculation for DE_RuS</b>	Season 1st	Season 2nd	Season 3rd
Biomass_WaPOR (kgDM/ha /season)	10697	11687	13650
Biomass_Flux (kgDM/ha /season)	13464	10098	16851
Water_Consumption_WaPOR (mm/season)	320	394	407
Water_Consumption_Flux (mm/season)	407	590	598
<b>GBWP_WaPOR (kgDM/m<sup>3</sup> H<sub>2</sub>O)</b>	<b>33.37</b>	<b>29.66</b>	<b>33.54</b>
<b>GBWP_Flux (kgDM/m<sup>3</sup> H<sub>2</sub>O)</b>	<b>33.08</b>	<b>17.12</b>	<b>28.18</b>

Table A 16. GBWP values with Flux dates for FR\_Aur

<b>GBWP calculation (Flux dates) for FR_Aur</b>	Season 1st	Season 2nd	Season 3rd	Season 4th
Biomass_WaPOR (kgDM/ha /season)	14088	11443	2667	
Biomass_Flux (kgDM/ha /season)	10736	12521	4455	5687
Water_Consumption_WaPOR (mm/season)	487	385	90	
Water_Consumption_Flux (mm/season)	442	388	51	212
<b>GBWP_WaPOR (kgDM/m<sup>3</sup> H<sub>2</sub>O)</b>	<b>28.93</b>	<b>29.72</b>	<b>29.64</b>	
<b>GBWP_Flux (kgDM/m<sup>3</sup> H<sub>2</sub>O)</b>	<b>24.29</b>	<b>32.27</b>	<b>87.36</b>	<b>26.83</b>

Table A 17. GBWP values with WaPOR dates for FR\_Aur

<b>GBWP calculation ( WaPOR dates) for FR_Aur</b>	Season 1st	Season 2nd	Season 3rd
Biomass_WaPOR (kgDM/ha /season)	15736	18842	16313
Biomass_Flux (kgDM/ha /season)	10916	12770	9375
Water_Consumption_WaPOR (mm/season)	547	694	628
Water_Consumption_Flux (mm/season)	478	524	347
<b>GBWP_WaPOR (kgDM/m<sup>3</sup> H<sub>2</sub>O)</b>	<b>28.77</b>	<b>27.15</b>	<b>25.98</b>
<b>GBWP_Flux (kgDM/m<sup>3</sup> H<sub>2</sub>O)</b>	<b>22.84</b>	<b>24.37</b>	<b>27.02</b>

Table A 18. GBWP values with respective dates for FR\_Aur

<b>GBWP calculation for FR_Aur</b>	Season 2nd	Season 3rd	Season 4th
Biomass_WaPOR (kgDM/ha /season)	11690	3321	10921
Biomass_Flux (kgDM/ha /season)	12508	4511	5880
Water_Consumption_WaPOR (mm/season)	394	114	422
Water_Consumption_Flux (mm/season)	395	62	268
<b>GBWP_WaPOR (kgDM/m<sup>3</sup> H<sub>2</sub>O)</b>	<b>29.67</b>	<b>29.14</b>	<b>25.88</b>
<b>GBWP_Flux (kgDM/m<sup>3</sup> H<sub>2</sub>O)</b>	<b>31.67</b>	<b>72.76</b>	<b>21.94</b>

Table A 19. GBWP values with Flux dates for FR\_Lam

<b>GBWP calculation (Flux dates) for FR_Lam</b>	Season 1st	Season 2nd	Season 3rd
Biomass_WaPOR (kgDM/ha /season)	17027	8982	7956
Biomass_Flux (kgDM/ha /season)	15223	16599	11220
Water_Consumption_WaPOR (mm/season)	565	345	239
Water_Consumption_Flux (mm/season)	556	412	289
<b>GBWP_WaPOR (kgDM/m<sup>3</sup> H<sub>2</sub>O)</b>	<b>30.14</b>	<b>26.04</b>	<b>33.29</b>
<b>GBWP_Flux (kgDM/m<sup>3</sup> H<sub>2</sub>O)</b>	<b>27.38</b>	<b>40.29</b>	<b>38.82</b>

Table A 20. GBWP values with WaPOR dates for FR\_Lam

<b>GBWP calculation ( WaPOR dates) for FR_Lam</b>	Season 1st	Season 2nd	Season 3rd
Biomass_WaPOR (kgDM/ha /season)	18622	16269	16780
Biomass_Flux (kgDM/ha /season)	15327	17060	12612
Water_Consumption_WaPOR (mm/season)	609	586	602
Water_Consumption_Flux (mm/season)	604	590	474
<b>GBWP_WaPOR (kgDM/m<sup>3</sup> H<sub>2</sub>O)</b>	<b>30.58</b>	<b>27.76</b>	<b>27.87</b>
<b>GBWP_Flux (kgDM/m<sup>3</sup> H<sub>2</sub>O)</b>	<b>25.38</b>	<b>28.92</b>	<b>26.61</b>

Table A 21. GBWP values with respective dates for FR\_Lam

<b>GBWP calculation for FR_Lam</b>	Season 1st	Season 2nd	Season 3rd
Biomass_WaPOR (kgDM/ha /season)	18622	11389	9824
Biomass_Flux (kgDM/ha /season)	15223	16488	11554
Water_Consumption_WaPOR (mm/season)	609	586	602
Water_Consumption_Flux (mm/season)	556	412	289
<b>GBWP_WaPOR (kgDM/m<sup>3</sup> H<sub>2</sub>O)</b>	<b>30.58</b>	<b>19.43</b>	<b>16.31</b>
<b>GBWP_Flux (kgDM/m<sup>3</sup> H<sub>2</sub>O)</b>	<b>27.38</b>	<b>40.02</b>	<b>39.98</b>

## REFERENCES

- Álvarez-Taboada, F., Tammadge, D., Schlerf, M., & Skidmore, A. (2015). Assessing MODIS GPP in Non-Forested Biomes in Water Limited Areas Using EC Tower Data. *Remote Sensing*, 7(3), 3274–3292. <https://doi.org/10.3390/rs70303274>
- Angus, J. F., & van Herwaarden, A. F. (2001). Increasing Water Use and Water Use Efficiency in Dryland Wheat. *Agronomy Journal*, 93(2), 290–298. <https://doi.org/10.2134/agronj2001.932290x>
- Balafoutis, A., Beck, B., Fountas, S., Vangeyte, J., Wal, T., Soto, I., Gómez-Barbero, M., Barnes, A., & Eory, V. (2017). Precision Agriculture Technologies Positively Contributing to GHG Emissions Mitigation, Farm Productivity and Economics. *Sustainability*, 9(8), 1339. <https://doi.org/10.3390/su9081339>
- Baldocchi, D. (2003). Assessing the eddy covariance technique for evaluating carbon dioxide exchange rates of ecosystems: past, present and future. *Global Change Biology*, 9(4), 479–492. <https://doi.org/10.1046/j.1365-2486.2003.00629.x>
- Baldocchi, D. (2014). Measuring fluxes of trace gases and energy between ecosystems and the atmosphere – the state and future of the eddy covariance method. *Global Change Biology*, 20(12), 3600–3609. <https://doi.org/10.1111/gcb.12649>
- Bastiaanssen, W. G. M., & Bos, M. G. (1999). Irrigation Performance Indicators Based on Remotely Sensed Data: a Review of Literature. *Irrigation and Drainage Systems*, 13(4), 291–311. <https://doi.org/10.1023/A:1006355315251>
- Blatchford, M. L., Mannaerts, C. M., Zeng, Y., Nouri, H., & Karimi, P. (2019). Status of accuracy in remotely sensed and in-situ agricultural water productivity estimates: A review. *Remote Sensing of Environment*, 234, 111413. <https://doi.org/10.1016/j.rse.2019.111413>
- Blum, A. (2009). Effective use of water (EUW) and not water-use efficiency (WUE) is the target of crop yield improvement under drought stress. *Field Crops Research*, 112(2–3), 119–123. <https://doi.org/10.1016/j.fcr.2009.03.009>
- Bossio, D., Geheb, K., & Critchley, W. (2010). Managing water by managing land: Addressing land degradation to improve water productivity and rural livelihoods. *Agricultural Water Management*, 97(4), 536–542. <https://doi.org/10.1016/j.agwat.2008.12.001>
- Cassman, K. G. (1999). Ecological intensification of cereal production systems: Yield potential, soil quality, and precision agriculture. *Proceedings of the National Academy of Sciences*, 96(11), 5952–5959. <https://doi.org/10.1073/pnas.96.11.5952>
- Chu, H., Luo, X., Ouyang, Z., Chan, W. S., Dengel, S., Biraud, S. C., Torn, M. S., Metzger, S., Kumar, J., Arain, M. A., Arkebauer, T. J., Baldocchi, D., Bernacchi, C., Billesbach, D., Black, T. A., Blanken, P. D., Bohrer, G., Bracho, R., Brown, S., ... Zona, D. (2021). Representativeness of Eddy-Covariance flux footprints for areas surrounding AmeriFlux sites. *Agricultural and Forest Meteorology*, 301–302, 108350. <https://doi.org/10.1016/j.agrformet.2021.108350>
- Clark, D. A., Brown, S., Kicklighter, D. W., Chambers, J. Q., Thomlinson, J. R., Ni, J., & Holland, E. A. (2001). Net primary production in tropical forests: An evaluation and synthesis of existing field data. In *Ecological Applications* (Vol. 11, Issue 2, pp. 371–384). Ecological Society of America. [https://doi.org/10.1890/1051-0761\(2001\)011\[0371:NPPITF\]2.0.CO;2](https://doi.org/10.1890/1051-0761(2001)011[0371:NPPITF]2.0.CO;2)
- Eugster, W., & Merbold, L. (2015). Eddy covariance for quantifying trace gas fluxes from soils. *SOIL*, 1(1), 187–205. <https://doi.org/10.5194/soil-1-187-2015>



- FAO and IHE Delft. (2019). *WaPOR quality assessment*.
- FAO and IHE Delft. (2020a). WaPOR database methodology. In *WaPOR database methodology*. FAO. <https://doi.org/10.4060/ca9894en>
- FAO and IHE Delft. (2020b). WaPOR V2 quality assessment – Technical Report on the Data Quality of the WaPOR FAO Database version 2. In *WaPOR V2 quality assessment – Technical Report on the Data Quality of the WaPOR FAO Database version 2*. FAO. <https://doi.org/10.4060/cb2208en>
- Ganeva, D., Tallec, T., Brut, A., Prikaziuk, E., Tomelleri, E., Koren, G., Verrelst, J., Berger, K., Graf, L. V., Belda, S., Cai, Z., & Silva, C. F. (2023). In-situ start and end of growing season dates of major European crop types from France and Bulgaria at a field level. *Data in Brief*, *51*, 109623. <https://doi.org/10.1016/j.dib.2023.109623>
- Gessese, A. A., & Melesse, A. M. (2019). Temporal relationships between time series CHIRPS-rainfall estimation and eMODIS-NDVI satellite images in Amhara Region, Ethiopia. In *Extreme Hydrology and Climate Variability* (pp. 81–92). Elsevier. <https://doi.org/10.1016/B978-0-12-815998-9.00008-7>
- Hellegers, P. J. G. J., Soppe, R., Perry, C. J., & Bastiaanssen, W. G. M. (2009). Combining remote sensing and economic analysis to support decisions that affect water productivity. *Irrigation Science*, *27*(3), 243–251. <https://doi.org/10.1007/s00271-008-0139-7>
- Huang, J., Gómez-Dans, J. L., Huang, H., Ma, H., Wu, Q., Lewis, P. E., Liang, S., Chen, Z., Xue, J.-H., Wu, Y., Zhao, F., Wang, J., & Xie, X. (2019). Assimilation of remote sensing into crop growth models: Current status and perspectives. *Agricultural and Forest Meteorology*, *276–277*, 107609. <https://doi.org/10.1016/j.agrformet.2019.06.008>
- Karunathilake, E. M. B. M., Le, A. T., Heo, S., Chung, Y. S., & Mansoor, S. (2023). The Path to Smart Farming: Innovations and Opportunities in Precision Agriculture. *Agriculture*, *13*(8), 1593. <https://doi.org/10.3390/agriculture13081593>
- Lasslop, G., REICHSTEIN, M., PAPALE, D., RICHARDSON, A. D., ARNETH, A., BARR, A., STOY, P., & WOHLFAHRT, G. (2009). Separation of net ecosystem exchange into assimilation and respiration using a light response curve approach: critical issues and global evaluation. *Global Change Biology*, *16*(1), 187–208. <https://doi.org/10.1111/j.1365-2486.2009.02041.x>
- Molden, D., Murray-Rust, H., Sakthivadivel, R., & Makin, I. (2003). A water-productivity framework for understanding and action. In *Water productivity in agriculture: limits and opportunities for improvement* (pp. 1–18). CABI Publishing. <https://doi.org/10.1079/9780851996691.0001>
- Nations, U., of Economic, D., Affairs, S., & Division, P. (2019). *World Population Prospects 2019 Highlights*.
- Pan, S., Tian, H., Dangal, S. R. S., Ouyang, Z., Tao, B., Ren, W., Lu, C., & Running, S. (2014). Modeling and Monitoring Terrestrial Primary Production in a Changing Global Environment: Toward a Multiscale Synthesis of Observation and Simulation. *Advances in Meteorology*, *2014*, 1–17. <https://doi.org/10.1155/2014/965936>
- Pastorello, G., Trotta, C., Canfora, E., Chu, H., Christianson, D., Cheah, Y. W., Poindexter, C., Chen, J., Elbashandy, A., Humphrey, M., Isaac, P., Polidori, D., Ribeca, A., van Ingen, C., Zhang, L., Amiro, B., Ammann, C., Arain, M. A., Ardö, J., ... Papale, D. (2020). The FLUXNET2015 dataset and the ONEFlux processing pipeline for eddy covariance data. *Scientific Data*, *7*(1). <https://doi.org/10.1038/s41597-020-0534-3>

- Ramoelo, A., Majozi, N., Mathieu, R., Jovanovic, N., Nickless, A., & Dzikiti, S. (2014). Validation of Global Evapotranspiration Product (MOD16) using Flux Tower Data in the African Savanna, South Africa. *Remote Sensing*, 6(8), 7406–7423. <https://doi.org/10.3390/rs6087406>
- Reichstein, M., Falge, E., Baldocchi, D., Papale, D., Aubinet, M., Berbigier, P., Bernhofer, C., Buchmann, N., Gilmanov, T., Granier, A., Grünwald, T., Havránková, K., Ilvesniemi, H., Janous, D., Knohl, A., Laurila, T., Lohila, A., Loustau, D., Matteucci, G., ... Valentini, R. (2005). On the separation of net ecosystem exchange into assimilation and ecosystem respiration: review and improved algorithm. *Global Change Biology*, 11(9), 1424–1439. <https://doi.org/10.1111/j.1365-2486.2005.001002.x>
- Safi, A. R., Karimi, P., Mul, M., Chukalla, A., & de Fraiture, C. (2022). Translating open-source remote sensing data to crop water productivity improvement actions. *Agricultural Water Management*, 261, 107373. <https://doi.org/10.1016/j.agwat.2021.107373>
- Sierra, C. A., Ceballos-Núñez, V., Hartmann, H., Herrera-Ramírez, D., & Metzler, H. (2022). *Ideas and perspectives: Allocation of carbon from Net Primary Production in models is inconsistent with observations of the age of respired carbon*. <https://doi.org/10.5194/egusphere-2022-34>
- Soussi, A., Zero, E., Sacile, R., Trincherro, D., & Fossa, M. (2024). Smart Sensors and Smart Data for Precision Agriculture: A Review. *Sensors*, 24(8), 2647. <https://doi.org/10.3390/s24082647>
- Tanner, C. B. (2015). *Measurement of Evapotranspiration* (pp. 534–574). <https://doi.org/10.2134/agronmonogr11.c30>
- The State of Food and Agriculture 2020. (2020). In *The State of Food and Agriculture 2020*. FAO. <https://doi.org/10.4060/cb1447en>
- Tilman, D., Balzer, C., Hill, J., & Befort, B. L. (2011). Global food demand and the sustainable intensification of agriculture. *Proceedings of the National Academy of Sciences*, 108(50), 20260–20264. <https://doi.org/10.1073/pnas.1116437108>
- Velpuri, N. M., Senay, G. B., Singh, R. K., Bohms, S., & Verdin, J. P. (2013). A comprehensive evaluation of two MODIS evapotranspiration products over the conterminous United States: Using point and gridded FLUXNET and water balance ET. *Remote Sensing of Environment*, 139, 35–49. <https://doi.org/10.1016/j.rse.2013.07.013>
- WaPOR database methodology*. (2020). FAO. <https://doi.org/10.4060/ca9894en>
- WaPOR quality assessment*. (2019). FAO and IHE Delft.
- Water for Sustainable Food and Agriculture A report produced for the G20 Presidency of Germany*. (n.d.). [www.fao.org/publications](http://www.fao.org/publications)
- Zhang, Y., Liu, H., Qi, J., Feng, P., Zhang, X., Liu, D. L., Marek, G. W., Srinivasan, R., & Chen, Y. (2023). Assessing impacts of global climate change on water and food security in the black soil region of Northeast China using an improved SWAT-CO2 model. *Science of The Total Environment*, 857, 159482. <https://doi.org/10.1016/j.scitotenv.2022.159482>
- Zhu, H., Lin, A., Wang, L., Xia, Y., & Zou, L. (2016). Evaluation of MODIS Gross Primary Production across Multiple Biomes in China Using Eddy Covariance Flux Data. *Remote Sensing*, 8(5), 395. <https://doi.org/10.3390/rs8050395>